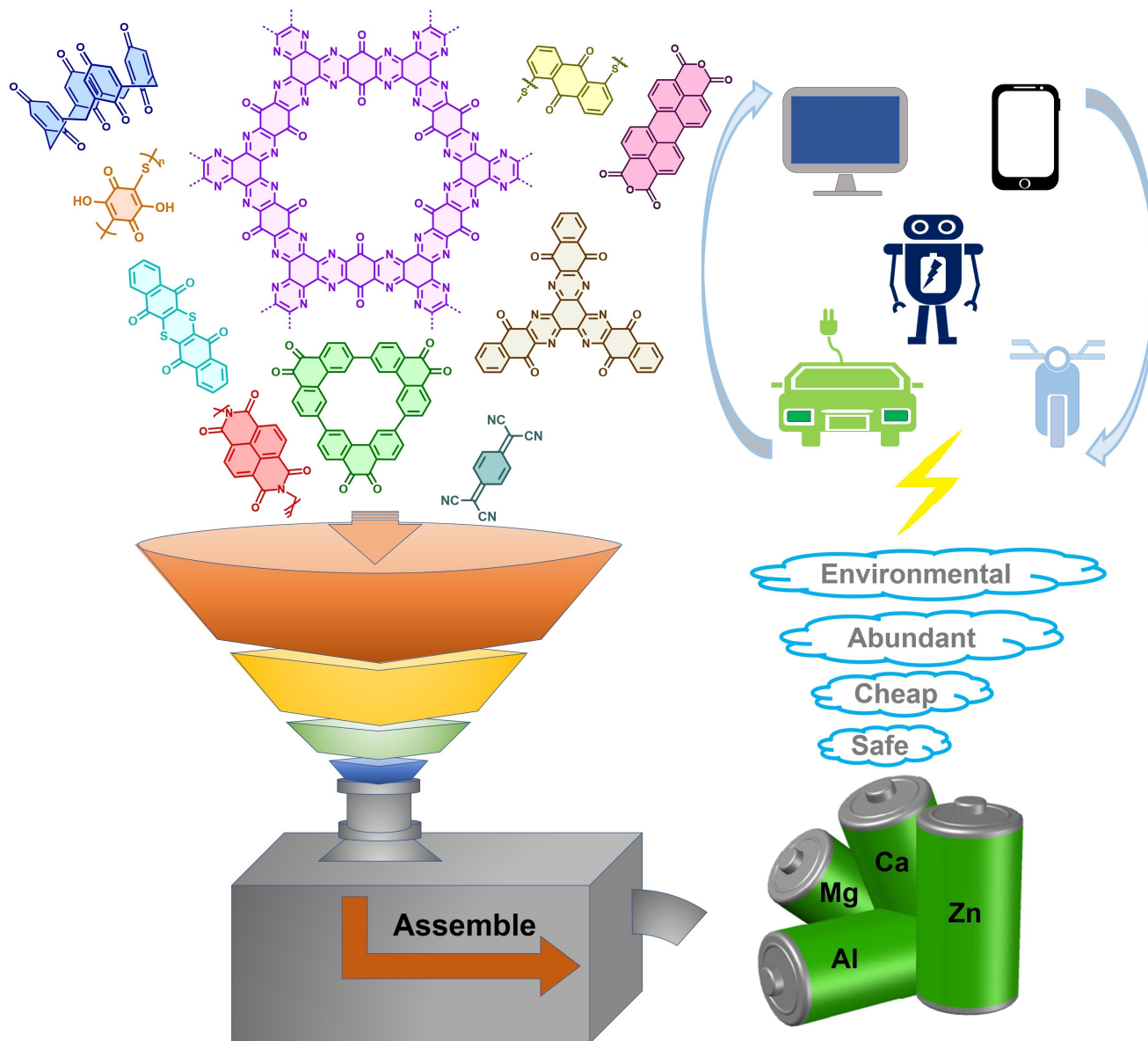


Special  
Collection

# Recent Progress on Organic Electrode Materials for Multivalent (Zn, Al, Mg, Ca) Secondary Batteries

Chaojian Ding<sup>+</sup><sup>[a]</sup>, Chaobo Li<sup>+</sup><sup>[a]</sup>, Hao Tian,<sup>[a]</sup> Yifan Tong,<sup>[a]</sup> Weiwei Huang,<sup>\*[a]</sup> and Qichun Zhang<sup>\*[b, c]</sup>



Multivalent secondary batteries (MSBs) have attracted great attention in view of their rich resources, low cost, and high safety. However, its development and application are still plagued by electrode materials. With their renewable and highly adjustable structures, organic electrode materials (OEMs) have several advantages over traditional inorganic electrode materials (IEMs), which has become the current research hotspot of electrode materials for MSBs. In this review, we present the recent developments in OEMs used for secondary batteries, including carbonyl compounds, imine compounds,

conductive polymers, covalent organic frameworks, organic cyanides, organosulfur polymers and so on. An overview of the structural characteristics, energy storage mechanism, and electrochemical performance of OEMs in MSBs is given. Furthermore, to reveal the reasons for the high performance of the preponderant organic electrode materials, the relationships between material structures, electrolyte system, and battery properties are discussed in detail. Finally, we hope that this review could provide a fundamental guide to developing and designing high-performance MSBs in the future.

## 1. Introduction

With the increasing environmental consciousness and the declining reserves of fossil energy, various forms of emerging renewable energy sources (such as solar energy, wind energy, tidal energy, geothermal energy, and biomass energy) have been rapidly demonstrated as alternatives.<sup>[1]</sup> However, their volatility and intermittent nature require that these energy sources must be stored centrally before using,<sup>[2]</sup> directly prompting the wide demand on low-cost, high-safety, and long-life energy storage devices. As one representative storage devices, lithium-ion batteries have been successfully commercialized in various energy-related equipment.<sup>[3]</sup> However, the low reserves and the uneven geographical distribution of resources make the price of lithium rising rapidly. Moreover, the highly-active nature of lithium provides lithium batteries the potential danger in practical applications. Thus, exploring novel reliable and safer rechargeable batteries is urgent and highly desirable.<sup>[4]</sup>

Multivalent metal resources (Zn, Al, Mg, Ca) have sparked extensive research interests in the development of multivalent secondary batteries (MSBs) due to their abundant reserves, low cost, and high energy density.<sup>[5]</sup> More importantly, Zn, Al and Mg show high safety in the air and conventional electrolytes. Therefore, MSBs have been regarded as one of the promising alternatives to lithium batteries. According to the previous reports,<sup>[6]</sup> the electrode materials of multivalent secondary batteries (MSBs) can be divided into three categories: inorganic

electrode materials (IEMs), organic electrode materials (OEMs) and their hybrid. IEMs are primarily vanadium-based,<sup>[7]</sup> molybdenum-based,<sup>[8]</sup> cobalt-based,<sup>[9]</sup> manganese-based oxides or sulfides,<sup>[10]</sup> as well as Prussian blue compounds,<sup>[11]</sup> where charge storages are achieved through the structural transformation of lattice and the change of valence state of metal centers.<sup>[12]</sup> However, inorganic compounds have limited room for further optimization due to lattice transition energy storage mechanisms. Meanwhile, the preparation of inorganic compounds is energy-intensive and frequently causes heavy pollution. Moreover, several researches have already indicated that the usage of IEMs as electrodes in MSBs is not consistent with the original intention of sustainable development. Thus, finding alternatives to replace IEMs is necessary. It is well known that OEMs have several superiorities including wide variety, a broad source of raw materials, low cost, and reproducibility, allowing them to be implemented in the storage of multivalent ions.<sup>[13]</sup> Different from IEMs, the core of energy storage in OEMs is the conversion and rearrangement of various active functional groups. The combination of different active functional groups endows OEMs with more flexible and changeable structures, resulting in a rich variety of active organic electrode materials.

Up to now, many organic small molecules containing carbonyl, amine, imine, and thioether have been successively employed as electrodes in MSBs.<sup>[14]</sup> Their charging/discharging mechanisms and characteristics are shown in Table 1. Meanwhile, various covalent organic frameworks (COFs) and conductive polymers based on the above-mentioned small molecules as building units have been continuously confirmed to improve the capacity and stability of MSBs. Even though some reviews on OEMs for the application in MSBs have been published,<sup>[15]</sup> comprehensive and systematic summaries on the latest advances of MSBs is rare.

To bridge the gap, we herein summarize the recent progress on OEMs for their application in MSBs, including secondary zinc batteries (SZBs), secondary aluminum batteries (SABs), secondary magnesium batteries (SMBs), and secondary calcium batteries (SCBs), where the structural characteristics, ions insertion, and electrochemical performance of various emerging organic electrode materials are introduced. In addition, the charge-discharge mechanism of various organic compounds is discussed in-depth as well. It is expected that this review will guide the subsequent development and design of the efficient OEMs as electrodes for the application in MSBs.

[a] C. Ding,<sup>+</sup> C. Li,<sup>+</sup> H. Tian, Y. Tong, Prof. W. Huang

School of Environmental and Chemical Engineering  
Yanshan University  
066004 Qinhuangdao, China

E-mail: huangweiwei@ysu.edu.cn

[b] Prof. Q. Zhang

Department of Materials Science and Engineering  
City University of Hong Kong  
SAR 999077 Hong Kong, China  
E-mail: qiczhang@cityu.edu.hk

[c] Prof. Q. Zhang

Center of Super-Diamond and Advanced Films (COSDAF)  
City University of Hong Kong  
SAR 999077 Hong Kong, China  
E-mail: qiczhang@cityu.edu.hk

[+] C. Ding, and C. Li contributed equally to this work.

An invited contribution to a Special Collection dedicated to Aqueous  
Electrolyte Batteries

**Table 1.** Summary of the energy storage mechanisms and characteristics of different types of organic electrode materials in MSBs.

Type	Redox mechanism	Example	Advantages	Disadvantages
Carbonyl compounds			high capacity fast kinetics	easy solubility low conductivity
Amine compounds			high conductivity	limited capacity unstable voltage plateau
Imine compounds			high capacity fast kinetics	easy solubility low conductivity
Nitrile compounds			fast kinetics	easy solubility low conductivity
Organosulfur compounds			high capacity	easy solubility low conductivity low kinetics



Chaojian Ding obtained his B.S. degree of chemical engineering and process at Tianjin University of Science and Technology in 2020. Now, he is a Master candidate at Yanshan University. His research focuses on the synthesis and fabrication of organic cathode materials for Zn-ion batteries.



Chaobo Li received his B.S. in polymer material and engineering from Xiangtan University in 2018. He is currently pursuing his Master's degree at Yanshan University. His major research interests focus on the synthesis and preparation of organic cathode materials for Zn batteries.



Hao Tian received his B.S. degree in molecular science and engineering from the North University of China in 2021. He is currently pursuing his Master's degree at Yanshan University. His research mainly focuses on the synthesis and preparation of organic cathode materials in Zn/Li batteries.



Yifan Tong received his B.Sc. degree in chemistry from Tianjin Normal University in 2019. Currently, he is pursuing the PhD candidate at Yanshan University. His research mainly focuses on the synthesis and preparation of organic cathode materials for Li/Na Batteries.



Weiwei Huang is a Professor at Yanshan University. She obtained her Ph.D. degree of physical chemistry at Nankai University in 2011. Then, she joined Prof. Jun Chen's group at Nankai University as a postdoctoral fellow. Since 2013, she joined the School of Environmental and Chemical Engineering at Yanshan University. She was a visiting scholar at Nanyang Technological University in 2019. Her research is focused on the organic electrode materials for Li/Na/K batteries.



Qichun Zhang received his B.S. at Nanjing University in China in 1992, MS in physical organic chemistry at Institute of Chemistry, Chinese Academy of Sciences in 1998, MS in organic chemistry at University of California, Los Angeles (USA, 2003), and completed his Ph.D. in chemistry at University of California Riverside in 2007. Then, he worked as a Postdoctoral Fellow (Oct. 2007–Dec. 2008) at Northwestern University. Since Jan. 2009, he joined School of Materials Science and Engineering at Nanyang Technological University (NTU, Singapore) as an Assistant Professor. On Mar 1st, 2014, he has promoted to Associate Professor with tenure. On Sep 1st, 2020, he moved to Department of Materials Science and Engineering at City University of Hong Kong as a full professor. From 2018 to 2021, he has been recognized as one of highly-cited researchers (top 1%) in cross-field in Clarivate Analytics. He is a fellow of the Royal Society of Chemistry. Currently, his research focuses on carbon-rich conjugated materials and their applications. Till now, he has published >455 papers and 5 patents (H-index: 97).

## 2. OEMs in SZBs

Benefiting from the relatively high energy density of zinc ( $5855 \text{ mAh cm}^{-3}$ ) and the +2 charge of its cation, aqueous SZBs are considered as a potential promising energy storage device.<sup>[16]</sup> Compared to organic electrolyte systems, aqueous electrolytes have the advantages of high safety, low preparation cost, and environmental friendliness.<sup>[17]</sup> Moreover, the mobility of ions in the water environment system is high, which can provide twice the ion conductivity of the organic electrolytes ( $\sim 1 \text{ Scm}^{-1}$ ).<sup>[18]</sup> Therefore, aqueous secondary zinc batteries (ASZBs) (developed based on aqueous electrolytes) have attracted researchers' extensive attention. Currently, a large number of organic compounds have been employed as electrodes in SZBs.<sup>[19]</sup> These materials can be mainly divided into conductive polymers, conjugate base compounds, imine compounds, covalent organic frame compounds, and so on.<sup>[20]</sup>

### 2.1. Conductive polymers

Conductive polymers are large  $\pi$ -conjugated systems, have high electrical conductivity, and could achieve ultra-high loadings greater than  $10 \text{ mg cm}^{-2}$ . Polyaniline (PANI) as the first conductive polymer is used in SZBs. Due to its deactivation problem in weakly acidic electrolytes, PANI exhibits poor cycling and rate performance.<sup>[21]</sup>

Shi et al. solved this issue by doping polyaniline electrode materials with sulfonic acid groups (Figure 1).<sup>[22]</sup> The doped  $-\text{SO}_3^-$  can store protons and ensure a locally high acidic environment. The sulfo-self-doped PANI (PANI-S) electrode displayed higher battery capacity performance and effective cycling life of over 2000 times in SZBs. Furthermore, Liu and Wang et al. reported the composites (PANI-VOH) of PANI and

$\text{V}_2\text{O}_5$  through an in-situ intercalation strategy.<sup>[23]</sup> The particular nanosheet structures of PANI-VOH provides rich reactive active sites for the reversible storage of  $\text{Zn}^{2+}$ , improving the electrochemical performance of PANI. Although SZBs based on polyaniline organic materials have shown great potential, they are still plagued by limited capacity and unstable voltage plateau. To overcome this problem, Zhang et al. developed poly(o-phenylenediamine) (PoPD) for SZBs.<sup>[24]</sup> During the charge/discharge process,  $\text{Zn}^{2+}$  could reversibly coordinate with the two conjugated  $\text{C}\equiv\text{N}$  bonds of the phenazine-like structures, achieving a stable charging and discharging platform. The as-fabricated SZBs based on PoPD showed good stability even after 3000 cycles at  $1 \text{ A g}^{-1}$ .

### 2.2. Conjugated carbonyl compounds

Relying on the reversible evolution between  $\text{C=O}$  and  $\text{C}-\text{O}^-$ , the conjugated carbonyl compounds can realize the  $\text{Zn}^{2+}$  storage through ionic coordination.<sup>[25]</sup> However, the electrochemical performance of carbonyl compounds in SZBs is limited by their low voltage platforms and the active material dissolution issue.

To address the problem of the structural instability of tetrachlorobenzoquinone (TCBQ) during charging and discharging, a strategy of embedding TCBQ molecules into carbon nanopores was proposed, effectively improving the cycling performance of Zn-TCBQ batteries.<sup>[26]</sup> Calix[4]quinone (C4Q), which has been previously developed for Li and Na batteries,<sup>[27]</sup> was also reported for SZBs recently.<sup>[28]</sup> From Figure 2(a and b), the SZBs deliver a discharge specific capacity as high as  $335 \text{ mAh g}^{-1}$  and an ultra-low polarization voltage. However, the capacity decay was still visibly observed during cycling. The Chen group overcame this challenge by using cationic proton-

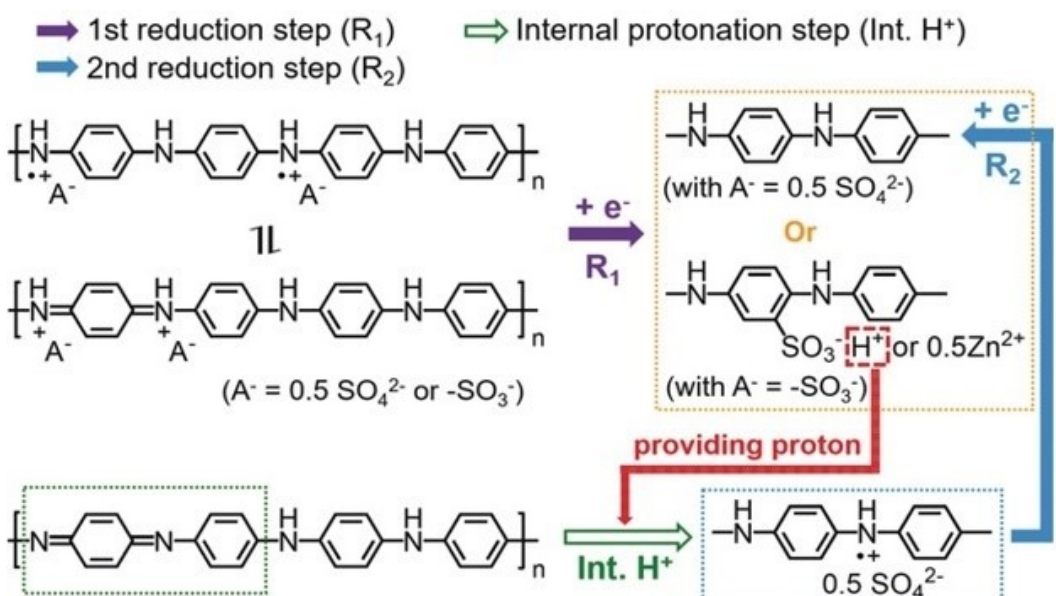
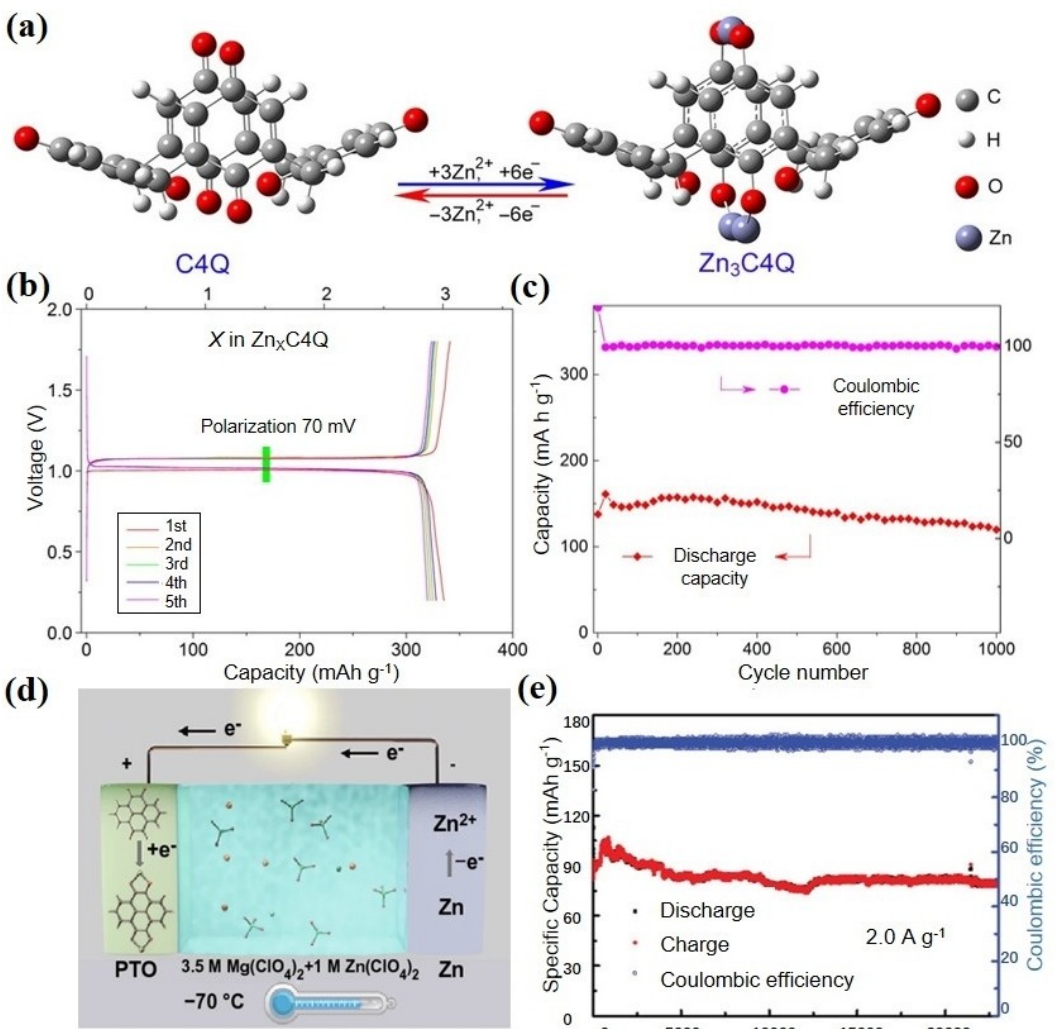


Figure 1. Reduction mechanism of the sulfo-self-doped PANI. Reproduced with permission from Ref. [22]. Copyright (2018) Wiley-VCH Verlag.



**Figure 2.** a) Optimized configurations of C4Q before and after  $\text{Zn}^{2+}$  uptake. b) Discharge-charge curves of Zn-C4Q battery. c) Cycling performance of Zn-C4Q batteries with a Nafion separator. Reproduced from Ref. [28]. Copyright (2018) The Author(s), American Association for the Advancement of Science. d) Schematic of low-temperature Zn-PTO battery. Reproduced from Ref. [30]. Copyright (2021) The Author(s). Published by Springer Nature. e) Cycling performance of Zn-DTT battery. Reproduced with permission from Ref. [29b]. Copyright (2020) Wiley-VCH Verlag.

exchange membranes (Nafion), achieving high cycling stability of 1000 cycles (Figure 2c).

Wang et al. have successively realized the application of pyrene-4,5,9,10-tetraone (PTO) and sulfur heterocyclic quinone dibenzo [b,i] thianthren-5,7,12,14-tetraone (DTT) in SZBs.<sup>[29]</sup> Using 2 M  $\text{ZnSO}_4$  as the electrolyte, the PTO electrode achieved a specific discharge capacity of 336 mAh g<sup>-1</sup>. In addition, the SZBs had an excellent low temperature ( $-70^\circ\text{C}$ ) stability in the electrolyte system of 3.5 M  $\text{Mg}(\text{ClO}_4)_2 + 1$  M  $\text{Zn}(\text{ClO}_4)_2$  as well (Figure 2d).<sup>[30]</sup> Another sulfur-containing organic molecule (DTT) has also successfully demonstrated excellent electrochemical stability in SZBs. Based on the synergistic storage mechanism of  $\text{H}^+$  and  $\text{Zn}^{2+}$ , the SZBs achieved a high specific capacity of 211 mAh g<sup>-1</sup> and an ultra-long lifetime (Figure 2e).

From the standpoint of molecular structures, organic molecules with rigid structures can effectively improve the cycling stability of electrode materials. The phenanthroline quinone macrocycle (PQ- $\Delta$ ) has a large conjugated carbonyl

structure, which could maintain the structural stability during charge and discharge processing (Figure 3a).<sup>[31]</sup> As shown in Figure 3(b and c), the insertion mechanism is confirmed through thermogravimetric analysis (TGA) and ex-situ Fourier Transform Infrared spectroscopy (FTIR). During the energy storage process, the insertion mechanism of hydrated  $\text{Zn}^{2+}$  effectively reduces the energy loss of desolvation between the electrode and electrolyte interface.

In order to obtain OEMs with high capacity and high stability, the polymerization of organic small molecule carbonyl compounds by the sulfur single bond is one of the effective strategies. Chen et al. synthesized polybenzoquinone sulfide (PBQS) with 2,5-dichloro-1,4-benzoquinone (DCBQ).<sup>[32]</sup> Thanks to the abundant electrochemical active sites of PBQS, the SZBs have an initial specific capacity of 203 mAh g<sup>-1</sup> at 0.1 C. Similarly, a sulfur dendritic polymer, poly(2,5-dihydroxy-1,4-benzoquinone sulfide) (PDBS), was subsequently reported to be applied to SZBs.<sup>[33a]</sup> The synthesis and charge-discharge mech-

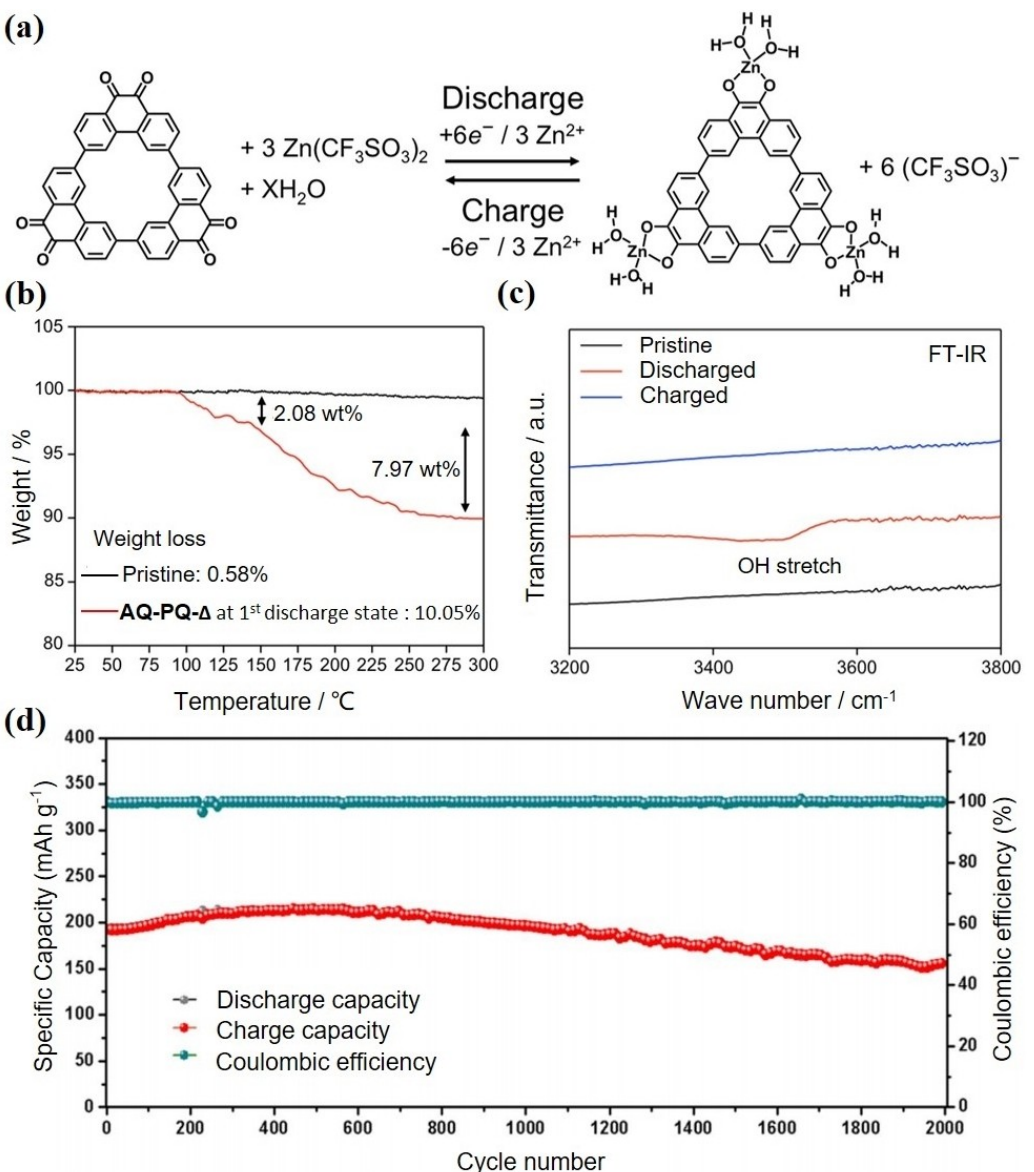


**Figure 3.** a) Redox mechanism of PQ- $\Delta$ . b) The TGA profiles and c) FT-IR spectra of PQ- $\Delta$  electrodes. Reproduced with permission from Ref. [31]. Copyright (2020) American Chemical Society. d) Cycling performance of Zn-PDBS battery. Reproduced with permission from Ref. [33a]. Copyright (2021) Wiley-VCH GmbH.

anism of PDBS are shown in Figure 4a. Different from monomeric CLA, the electrode material has some problems, such as fast dissolution rate and capacity fading.<sup>[34]</sup> The introduction of S heteroatoms in PDBS enhances the electron-donating effect on the electrochemical reactivity of the cathode materials. The Zn-PDBS battery exhibited extremely high cycling stability (capacity retention was still 79% after up to 2000 cycles at a large current density of  $2\text{ A g}^{-1}$ ) (Figure 3d).

### 2.3. Imine compounds

Except for carbonyl compounds, imine( $\text{C}=\text{N}$ )-based organic materials are highly electronegative and show high redox activity. As reported by the Niu group, a novel zinc organic

battery with diquinoxalino [2,3-a:2',3'-c] phenazine (HATN) as the cathode was developed.<sup>[35]</sup> The Zn-HATN battery not only exhibited an initial discharge capacity of  $405\text{ mAh g}^{-1}$  at  $100\text{ mA g}^{-1}$  but also had a high capacity retention rate. However, the Zn-HATN battery still suffers from the problem of low operating voltage.

Ye et al. overcame the above challenge by introducing three strong electron-absorbing groups ( $-\text{CN}$ ) into HATN.<sup>[36]</sup> As shown in Figure 4b, compared with HATN, the introduction of  $-\text{CN}$  reduces the lowest unoccupied molecular orbital (LUMO) energy of HATN-3CN and enhances the electron affinity. The modified HATN-3CN electrode displayed excellent rate capability and long cycle life at  $5\text{ A g}^{-1}$  (the capacity retention rate was up to 90.7% after 5800 cycles). In order to further improve the electrochemical performance of HATN, a small molecule

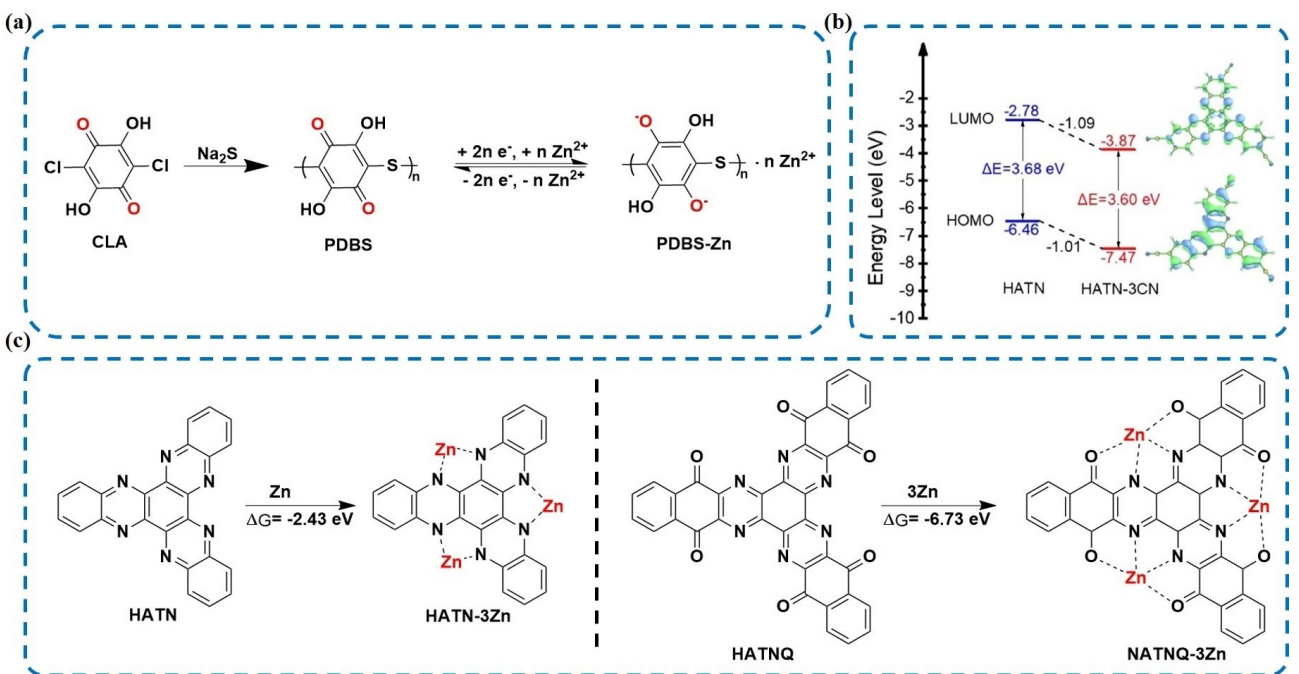


**Figure 4.** a) Proposed redox mechanism for SZBs. Reproduced with permission from Ref. [33a]. Copyright (2021) Wiley-VCH GmbH. b) The energy diagrams of HATN and HATN-3CN. Reproduced with permission from Ref. [36]. Copyright (2021) Elsevier B.V. c) Binding Gibbs free energy for HATN and HATNQ with zinc cation stage. Reproduced with permission from Ref. [37]. Copyright (2022) Wiley-VCH GmbH.

hexaaazatrifluorophthalene-quione (HATNQ) with multiple C=O and C=N active groups was developed based on HATN.<sup>[37]</sup> The unique 2D supramolecular structure of HATNQ and the existence of hydrogen bonds enhance the storage capacity for Zn<sup>2+</sup> and H<sup>+</sup>. The Zn-HATNQ battery achieved an excellent specific discharge capacity of 483 mAh g<sup>-1</sup> at 0.2 A g<sup>-1</sup>. The theoretical calculation indicates that the presence of oxygen atoms makes the structure of O...Zn...N much stable, greatly enhancing the coordination ability of HATNQ with Zn<sup>2+</sup> as well (Figure 4c).

Pyrazine is one of the typical structures containing C=N functional groups, which can provide stable active sites for the storage of Zn<sup>2+</sup> as well. The Song team synthesized a multi-active-site organic compound TAPQ with a quinone/pyrazine structure through ingenious molecular design.<sup>[38]</sup> Similar to HATNQ, TAPQ has two electrochemically active sites: C=O and C=N, enabling reversible storage of Zn<sup>2+</sup> and H<sup>+</sup> in aqueous electrolytes.

#### 2.4. Covalent organic frameworks

Covalent organic frameworks (COFs) have rich pore structure, ultra-high specific surface area, and good thermal stability, showing an excellent application value in the field of electrochemical energy storage.<sup>[39]</sup> Khayum et al. firstly reported a hydroquinone-based COF (HqTp) as a cathode material for water-based SZBs (Figure 5a).<sup>[40]</sup> As shown in Figure 5(b and c), HqTp-COF has a well-defined nanopores structure. Meanwhile, the strong and reversible interactions between C=O and Zn or Zn and N-H among adjacent layers of COFs could be clearly

investigated. Based on the above-mentioned structural characteristics, the HqTp-COF electrode could achieve rapid reaction kinetics and an initial discharge capacity of 125 mAh g<sup>-1</sup>.

In 2020, an organic covalent compound (PA-COF) with the adjacent Philoline functional group as the electrochemical active site was synthesized by Wang et al. (Figure 6a).<sup>[41]</sup> Using inductively coupled plasma atomic emission spectroscopy and solid-state nuclear magnetic resonance (NMR), the co-intercalation and extraction mechanism of Zn<sup>2+</sup> and H<sup>+</sup> was confirmed (Figure 6b and c). The Zn-PA-COF battery could achieve a long cycle life of up to 10000 cycles with small decay rates.

Whereafter, Wang et al. developed another new COF material HAQ-COF again by grafting quinone onto 1,4,5,8,9,12-hexaaazatriphenylene-based COFs.<sup>[42]</sup> HAQ-COF provides more active sites for Zn<sup>2+</sup> complexation and achieves the coordination of O...Zn...N. In addition, the introduction of carbonyl groups makes the electron delocalization range of the HAQ-COF framework larger, showing higher redox activity (Figure 6d). Consequently, the SZBs delivered a high discharge specific capacity of 344 mAh g<sup>-1</sup> at a current density of 0.1 A g<sup>-1</sup>. As discussed above, COFs with ordered, porous and multi-active sites have great application potential as zinc organic cathode materials.

#### 3. OEMs in SABs

As the highest content of the metal element in the crust, aluminum (Al) has a high gravimetric capacity (2980 mAh g<sup>-1</sup>) and volume capacity (8045 mA cm<sup>-3</sup>).<sup>[43]</sup> In addition, the standard electrode potential (vs standard hydrogen electrode)

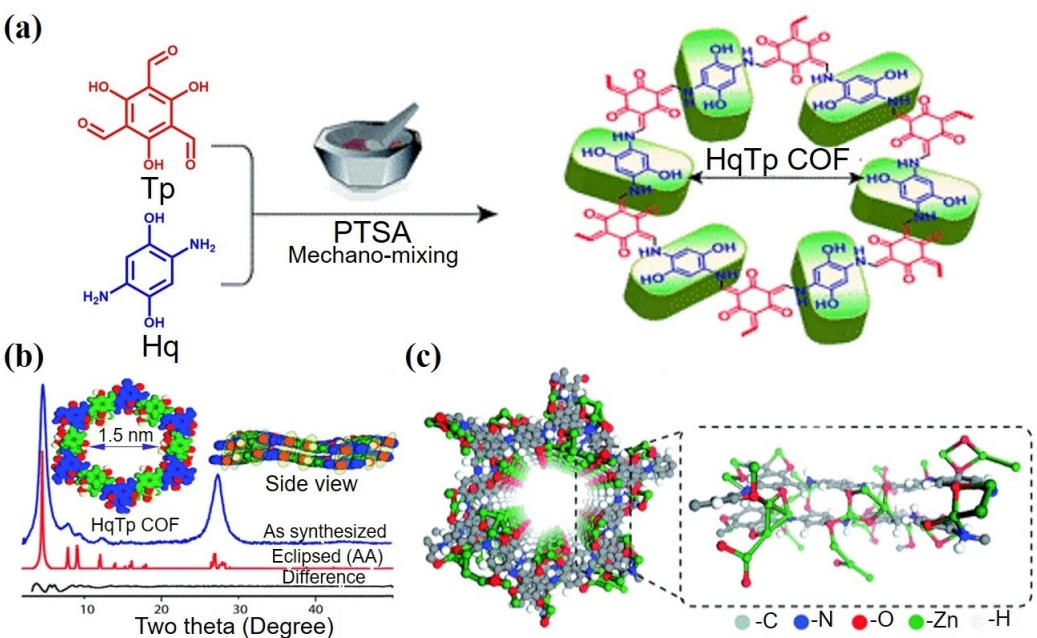


**Figure 5.** a) Schematic representation of the synthesis of HqTp. b) The XRD pattern with slipped SCC-DFT model. c) The DFTB model of interlayer interaction of Zn<sup>2+</sup> cations with the adjacent layers of HqTp. Reproduced from Ref. [40]. Copyright (2019) The Royal Society of Chemistry with CC BY-NC 3.0.

(SHE) of Al element is 1.68 V, making SABs relatively safe among metal-ion batteries. Therefore, SABs are emerging batteries with great development potential.<sup>[44]</sup> However, SABs are not stable in traditional aqueous electrolytes and may generate some by-products, such as Al<sub>2</sub>O<sub>3</sub> and H<sub>2</sub>,<sup>[45]</sup> which seriously affects the cycle life of batteries. Fortunately, the introduction of ionic liquid (IL) electrolytes helps to alleviate the above issues while also improving the performance of SABs.<sup>[46]</sup> Up to now, the reported OEMs in SABs are dominated by the anode materials. They can be divided into the following categories: inorganic-organic composites, carbonyl compounds, and polymer/conductive carbon composites.

### 3.1. Inorganic-organic composites

Inorganic metal-containing compounds such as metal chalcogenides and metal oxides have been sought by the reason of their high theoretical capabilities. However, the electrochemical reversibility of electrode materials is poor during the cycle process, and the cycling stability of the battery needs to be further improved.<sup>[47]</sup>

Synthesizing composite materials (such as conductive carbon, organics, etc.) or improving the interface design of motor materials are feasible to approach high stability.<sup>[48]</sup> As recently reported,<sup>[49]</sup> MoS<sub>2</sub>/polythiophene (MoS<sub>2</sub>/PTh) composite cathodes were created via *in situ* thiophene polymerization, delivering a higher capacity and cycling performance than that of individual MoS<sub>2</sub> or PTh cathode. The MoS<sub>2</sub>/PTh cathode had an initial capacity of up to 150 mAh g<sup>-1</sup>. Xiao et al. prepared a MOF-derived Co<sub>3</sub>O<sub>4</sub>@MWCNTs polyhedral composite.<sup>[50]</sup> Its unique polyhedral morphology and large specific surface area

provide high electronic conductivity and strong internal microstructure, allowing that the composite electrode has excellent electrochemical performance.

### 3.2. Carbonyl compounds

Electrochemically active organic molecules usually have more flexible redox structures. Especially in the intercalation/deintercalation process of multivalent Al<sup>3+</sup>, where the molecule has less irreversible deformation, more stable electrochemical properties can be achieved. Note that organic compounds containing carbonyl groups are still the most commonly used compounds as electrodes in SABs until now.

9,10-Anthraquinone (AQ) has been reported as an aluminum battery electrode that achieved reversible extraction and insertion of Al<sup>3+</sup> with an excellent capacity retention (89.4%) (Figure 7a).<sup>[51]</sup> During the same period, Yan et al. also researched SABs of AQ/K<sub>2</sub>CuFe(CN)<sub>6</sub>.<sup>[52]</sup> Although the initial discharge capacity of the full battery is only 53 mAh g<sup>-1</sup>, it could provide theoretical guidance for the design of such SABs (Figure 7b).

Analogous to SZBs, the dissolution of small organic molecules into electrolytes in SABs is also an inevitable problem, seriously affecting the stability of the battery during long cycles. The optimization of organic molecular structures or the formation of multimeric structures with special groups is a feasible approach. In 2019, Kim et al. synthesized PQ triangle (PQ-Δ) using phenanthrenequinone (PQ) as a monomer in SABs.<sup>[53]</sup> The layered structure of the PQ-Δ rigid triangular macrocycle led to reduce solvent effects, significantly promoting the specific capacity and cycling stability of SABs.

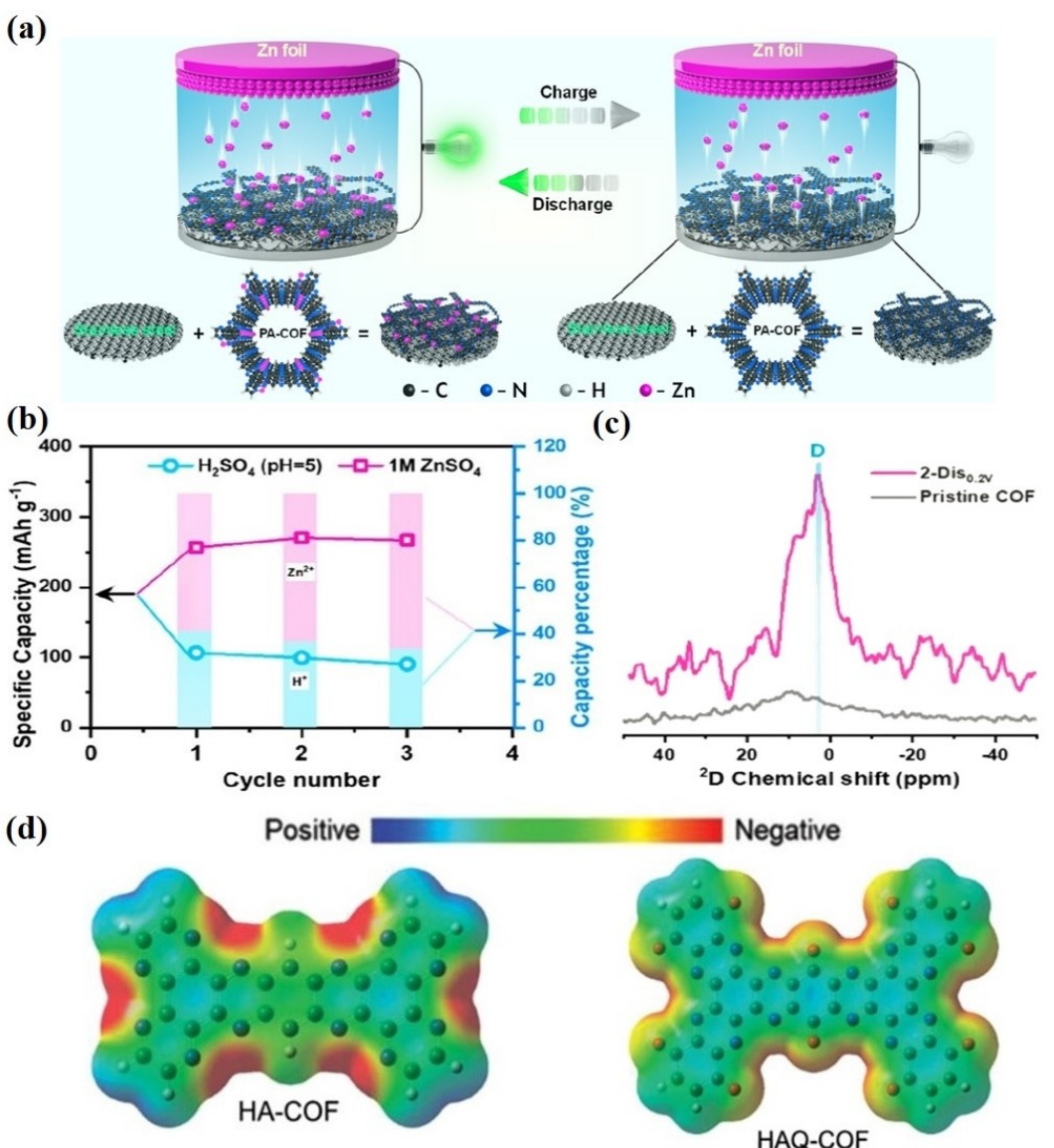


**Figure 6.** a) Schematic configuration of Zn-PA-COF battery. b) Quantitative analysis of  $\text{Zn}^{2+}$  and  $\text{H}^+$  contributions to capacity. c) Comparative deuterium (<sup>2</sup>D) solid-state NMR spectra. Reproduced from Ref. [41]. Copyright (2020) American Chemical Society with CC-BY license. d) Electrostatic potential surface of COF showing possible active sites. Reproduced from Ref. [42]. Copyright (2021) Wiley-VCH GmbH.

Subsequently, 1,4-benzoquinone (TPB) was studied as a cathode material for SABs.<sup>[54]</sup> The presence of four bulky phthalimide groups effectively inhibits its dissolution. In addition, the active sites adjacent to molecules also readily bind to multivalent ions. In Figure 8(a), Al-TPB batteries (urea electrolyte) show good rate performance. As a macrocyclic molecule, the multi-adjacent carbon-based and large cavity structure of C4Q not only inhibits its dissolution but also facilitates the intercalation of multivalent ions. Li et al. optimized the C4Q structure to become excellent cathode materials for high-energy-density SABs.<sup>[55]</sup> In Figure 8(b), the modification C4Q electrode shows excellent temperature performance in the  $\text{Al}(\text{OTf})_3$  electrolyte. The research is expected to broaden the battery applications. Moreover, the Fang group synthesized the sulfurized polymer PTCDA-SP by

introducing a sulfinyl group ( $-\text{S}-$ ) into PTCDA.<sup>[56]</sup> The cycling performances of the two electrodes are shown in Figure 8(d), the capacity of PTCDA-SP electrodes was still stable above  $100 \text{ mA g}^{-1}$  even after 1200 cycles. However, the capacity of the PTCDA electrode displayed a sharp drop in the first few dozen cycles. This example fully demonstrates the advantages of bridging  $-\text{S}-$  bonds: the bridged sulfide bond in the polymer molecular structure endows polysulfide with strong flexibility and effectively inhibits the dissolution of active substances, thus enhancing the cycling stability of the battery (Figure 8c).

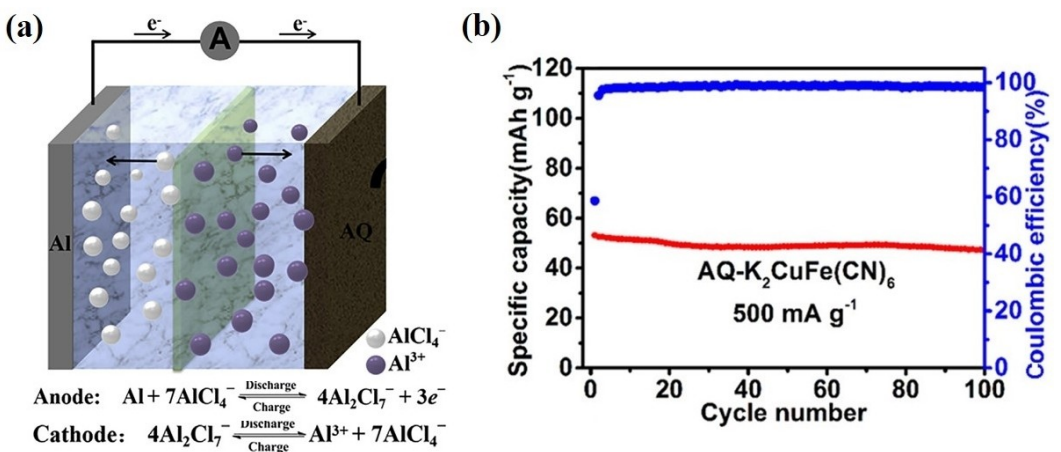


**Figure 7.** a) Schematic illustration of the rechargeable aluminum battery with AQ. Reproduced from Ref. [51]. Copyright (2021) The Author(s). Published by Elsevier with CC BY-NC-ND license. b) Cycling performance of the AQ/ $\text{K}_2\text{CuFe}(\text{CN})_6$  full battery. Reproduced from Ref. [52]. Copyright (2021) American Chemical Society.

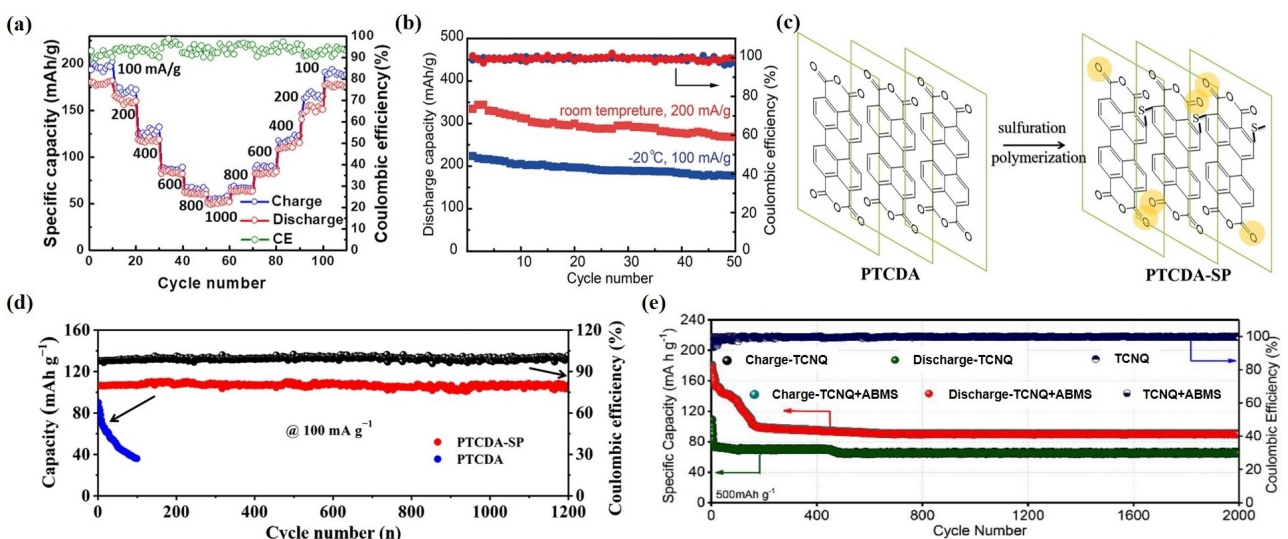


**Figure 8.** a) Rate capability of the Al-TPB battery. Reproduced with permission from Ref. [54]. Copyright (2020) American Chemical Society. b) Cycling performance of Al-C4Q battery at different temperatures. Reproduced with permission from Ref. [55]. Copyright (2020) Wiley-VCH GmbH. c) Schematic diagram of the synthesis process and active site arrangement of PTCDA-derived polymer. d) Cycling performance of the PTCDA and PTCDA-SP. Reproduced with permission from Ref. [56]. Copyright (2021) Science Press and Dalian Institute of Chemical Physics, Chinese Academy of Sciences. Published by Elsevier B.V. and Science Press. e) Cycling performance of TCNQ in the Al batteries with and without acetylene black modified separator. Reproduced with permission from Ref. [58]. Copyright (2020) Elsevier B.V.

### 3.3. Imine compounds and organic cyanides

Except for the organic molecules with carbonyl groups as active materials for aluminum batteries, organic molecules with C=N and C≡N also have also been reported for the applications in aluminum batteries, for example, PHATN formed from the polymerization of the organic molecule HATN. Inspired by the reversible storage capacity of Mg<sup>2+</sup>, Mao et al. used PHATN as the positive electrode of SABs to explore the Al<sup>3+</sup> storage capacity.<sup>[57]</sup> The results showed that the battery had an initial discharge capacity of 145 mAh g<sup>-1</sup> at 50 mAh g<sup>-1</sup>. However, the capacity of the battery was reduced to 92 mAh g<sup>-1</sup> after 100 cycles.

The C≡N has greater electron affinity than C=O, exhibiting stronger redox activity. Therefore, organic molecules with cyanogenic groups are also potential cathode materials in SABs. When tetracyanoquinodimethane (TCNQ), tetracyanoethylene (TCNE), and tetrakis(4-cyanophenyl)methane (TCPM) as anode materials, Guo et al. found that the highly polar cyanide groups in the molecule can act as redox-active sites for reversible coordination/dissociation with AlCl<sub>3</sub><sup>+</sup>.<sup>[58]</sup> Among them, TCNQ had an initial capacity of 180 mAh g<sup>-1</sup> at 500 mA g<sup>-1</sup>. Furthermore, the modified TCNQ+ABMS composite electrode maintained a coulombic efficiency of around 100% after 2000 cycles (Figure 8e).

### 3.4. Polymer/conductive carbon composites

Benefiting from the multiple active sites in the polymer chains and the fast charge transport rate provided by conductive carbon, polymer/conductive carbon materials often exhibit superior electrochemical performance than single polymers. Kong et al. developed the Pth@GO composite electrode material, demonstrating a higher capacity than Pth and GO (Figure 9a).<sup>[59]</sup> Based on the storage mechanism of strong electrostatic interaction between charge carriers and the C<sub>β</sub>-H sites of the Pth chain, the Pth@GO-Al battery displays a high discharge capacity of 130 mAh g<sup>-1</sup> at 1 A g<sup>-1</sup>, with excellent rate performance and cycling stability (Figure 9b).

In 2020, the G-PANI composite material was synthesized for the first time and applied as a cathode in SABs. The SABs assembled by G-PANI displayed a performance far exceeding that of similar materials.<sup>[60]</sup> After 4000 cycles, the discharge capacity still reached 180 mAh g<sup>-1</sup> at 1000 mA g<sup>-1</sup>. The rate performance of the battery was extremely excellent at a high current density as well. Furthermore, it was also confirmed that the charge storage mechanism of polyaniline depended on the moderate interaction between the –NH in the polyaniline chain and electrolyte anions, such as AlCl<sub>4</sub><sup>-</sup>.

## 4. OEMs in SMBs

SMBs are known as a promising candidate for energy storage due to their high volumetric capacity, safety, and reversible dendrite-free Mg deposition.<sup>[61]</sup> However, the strong electrostatic interaction between highly polar Mg<sup>2+</sup> and electrode materials leads to slow diffusion kinetics, seriously affecting the performance of batteries. Therefore, it is particularly important to develop suitable cathode materials for SMBs.<sup>[62]</sup> Organic materials have been gradually applied in the research of SMBs due to their environmental friendliness and highly designable

ability.<sup>[63]</sup> They mainly include carbonyl compounds, conductive polymers, imine polymers, and organosulfur compounds.

### 4.1. Carbonyl compounds

Carbonyl compounds, widely explored as OEMs in LIBs, are universal electrode materials in SMBs as well. As typical quinone monomers with a conjugated structure, anthraquinone (AQ), 1,4-nathalquinone (NQ), and 1,4-phenylquinone (BQ) have been reported as cathode materials for SMBs.<sup>[64]</sup> In Figure 10(a), the initial capacities of AQ, NQ, and BQ are 152 mAh g<sup>-1</sup>, 138 mAh g<sup>-1</sup>, and 130 mAh g<sup>-1</sup>, respectively. However, the capacities of these three materials decay rapidly in subsequent cycles, arising from the dissolution of small molecules in electrolytes. Therefore, maintaining the stability of electrode materials is particularly important to improve the long-cycling performance of SMBs.

To further investigate the effect of the conjugated structures of organic compounds on the performance of magnesium batteries, three different degrees of conjugated acid anhydrides were selected.<sup>[65]</sup> Surprisingly, 3,4,9,10-perylene-tetracarboxylic dianhydride with larger conjugated facets displayed higher Mg<sup>2+</sup> storage capacity and better cycling stability in practice, which was the opposite of the theoretical capacity (Figure 10b). Ex-situ X-ray photoelectron spectroscopy (XPS) analysis demonstrated that the large conjugated structure of PTCDA enhanced the carbonyl enolization and played a more important role in the reversible storage capacity of Mg<sup>2+</sup>.

Reasonably ameliorating the electrical conductivity of organic materials can effectively improve the performance of SMBs. Xiu et al. prepared poly(1,4-anthraquinone)/Ketjenblack (14PAQ@KB) by solution dispersion.<sup>[66]</sup> The addition of conductive carbon effectively improves the cathode-electrolyte interface and facilitates the transfer of charge and ion. As shown in Figure 10(c), 14PAQ@KB electrode exhibits the

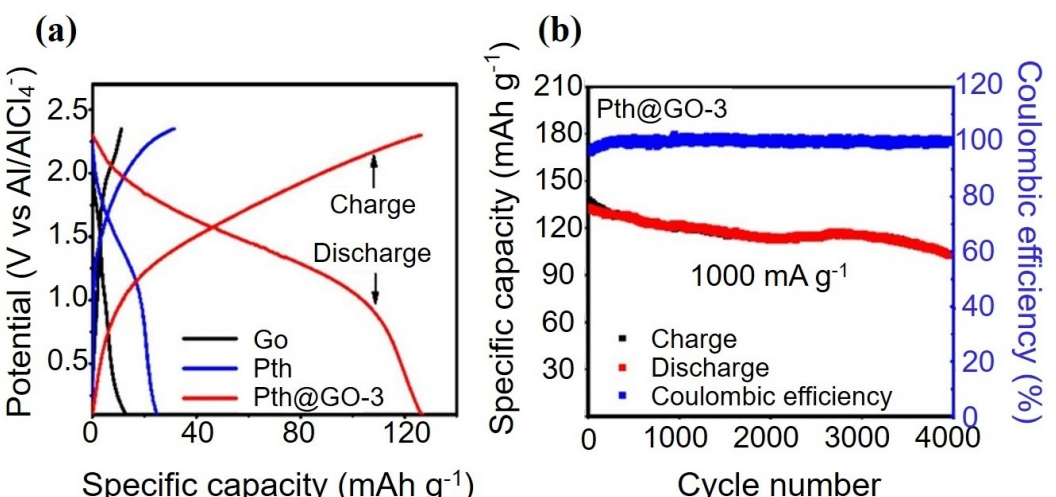
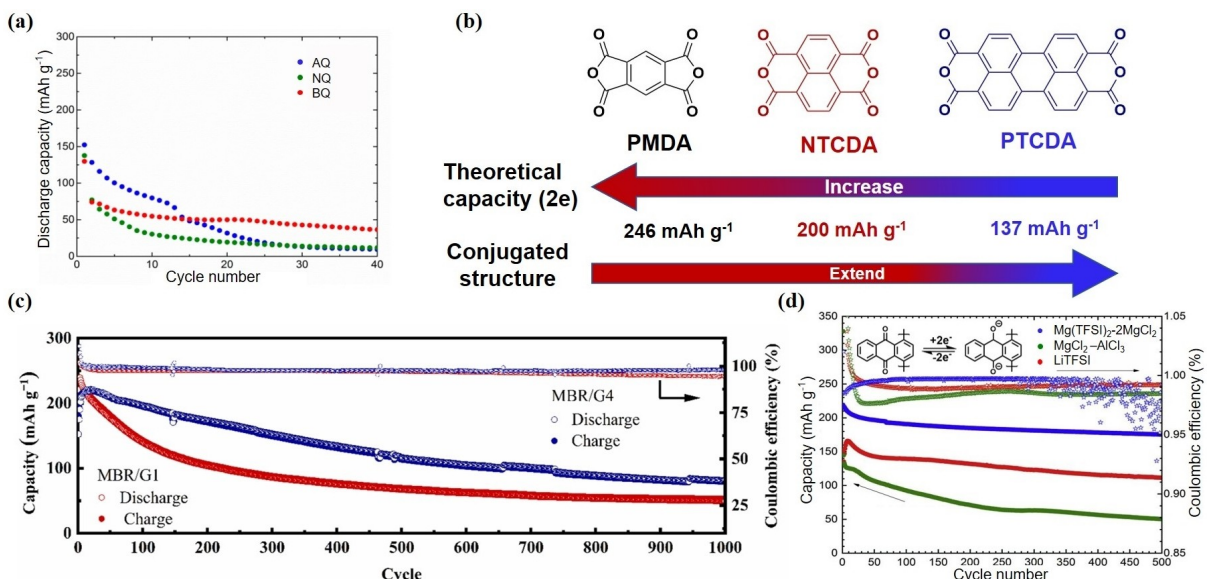


Figure 9. a) Discharge-charge curves of GO, Pth, and Pth@GO-3. b) Cycling performance of Pth@GO-3. Reproduced with permission from Ref. [59]. Copyright (2020) American Chemical Society.



**Figure 10.** a) Discharge curves of AQ, NQ, and BQ. Reproduced from Ref. [64]. Copyright (2020) The Author(s), published by Multidisciplinary Digital Publishing Institute. b) Structures with theoretical capacities of PMDA, NTCDA, and PTCDA. Reproduced with permission from Ref. [65]. Copyright (2021) Wiley-VCH GmbH. c) Cycling performance of 14PAQ@KB. Reproduced with permission from Ref. [66]. Copyright (2021) Wiley-VCH GmbH. d) Cycling performance of PAQ in  $\text{Mg}(\text{TFSI})_2\text{-}2\text{MgCl}_2$  and  $\text{MgCl}_2\text{-}\text{AlCl}_3$ . Reproduced with permission from Ref. [68]. Copyright 2019, Elsevier.

capacity of  $81 \text{ mAh g}^{-1}$  after 1000 cycles, which is better than that of 14PAQ.<sup>[67]</sup>

Furthermore, an appropriate electrolyte system is particularly critical to the performance of SMBs. In 2019, the electrochemical properties of polyanthraquinone (PAQ) were investigated in two different electrolytes.<sup>[68]</sup> The result showed that PAQ in  $\text{Mg}(\text{TFSI})_2\text{-}2\text{MgCl}_2$  electrolyte had better charge and discharge reversibility and fast reaction kinetics (Figure 10d).

By adding a soluble salt (1 M LiCl) to the electrolyte, Lian et al. improved the utilization efficiency of active materials.<sup>[69]</sup> The PTCDA electrode delivers a higher magnesium storage capacity and excellent cycling performance (Figure 11a).

## 4.2. Conductive polymers

Polyaniline (PANI) is considered as a potential raw part of electrode materials for SMBs because of its low cost, high conductivity, and excellent stability.<sup>[70]</sup> Zuo et al. developed 2D organic-inorganic superlattice cathode material PANI-V<sub>2</sub>O<sub>5</sub> (PVO) by compositing PANI with V<sub>2</sub>O<sub>5</sub>.<sup>[71]</sup> The embedding of PANI in the interlayer region of V<sub>2</sub>O<sub>5</sub> not only significantly reduced the electrostatic interaction between Mg<sup>2+</sup> and V<sub>2</sub>O<sub>5</sub> but also provided more charge storage sites. Based on these advantages, PVO showed excellent cycling stability (80 mAh g<sup>-1</sup> after 500 cycles at  $4 \text{ A g}^{-1}$ ) and a higher capacity (280 mAh g<sup>-1</sup> at  $100 \text{ mA g}^{-1}$ ) (Figure 11b).

## 4.3. Imine polymers

Recently, imine polymers with C=N functional groups have been proven to be active sites for the reversible storage of

Mg<sup>2+</sup>. Inspired by the excellent electrochemical performance of PHATN in sodium batteries, Mao et al. continued to try to use PHATN as an electrode for SMBs.<sup>[57]</sup> PHATN delivered a reversible capacity of  $110 \text{ mAh g}^{-1}$  after 200 cycles and an excellent rate performance (Figure 12a and b). XPS, FTIR, Raman spectra, and density functional theory (DFT) calculations also further displayed that the C=N bond in PHATN could realize the reversible storage of Mg<sup>2+</sup>. COF material had a larger surface area and more pore structure, which can effectively promote the diffusion of Mg<sup>2+</sup>. A triazine-based porous COF cathode material was firstly applied to magnesium storage by Sun et al.<sup>[72]</sup> Ex-situ XPS analysis demonstrated that the triazine ring in COF was the redox center for the reversible reaction of Mg<sup>2+</sup>, and each COF repeating unit could reversibly combine with multiple Mg<sup>2+</sup> (Figure 12c). This unique triazine ring structure enables COF materials to operate under high current density conditions with minimal capacity decay rate (Figure 12d). The triazine ring COF material has excellent electrochemical properties and provides a new direction for the development of organic positive SMBs.

## 4.4. Organosulfur compounds

The introduction of S atoms into organic compounds can improve the reaction kinetics and enhance the stability of active substances to a certain extent.<sup>[73]</sup> As a new anode material, sulfur-3,4,9,10-perylene-tetracarboxylate (PTC-S) was prepared by ring-opening sulfide grafting based on PTCDA by Cang et al.<sup>[74]</sup> Meanwhile, they also successfully assembled a novel aqueous Mg–Li dual-ion battery using dual-ion electrolytes (0.5 M LiCl and 0.5 M MgCl<sub>2</sub>). This research effectively broadens the electrochemical window and improves the

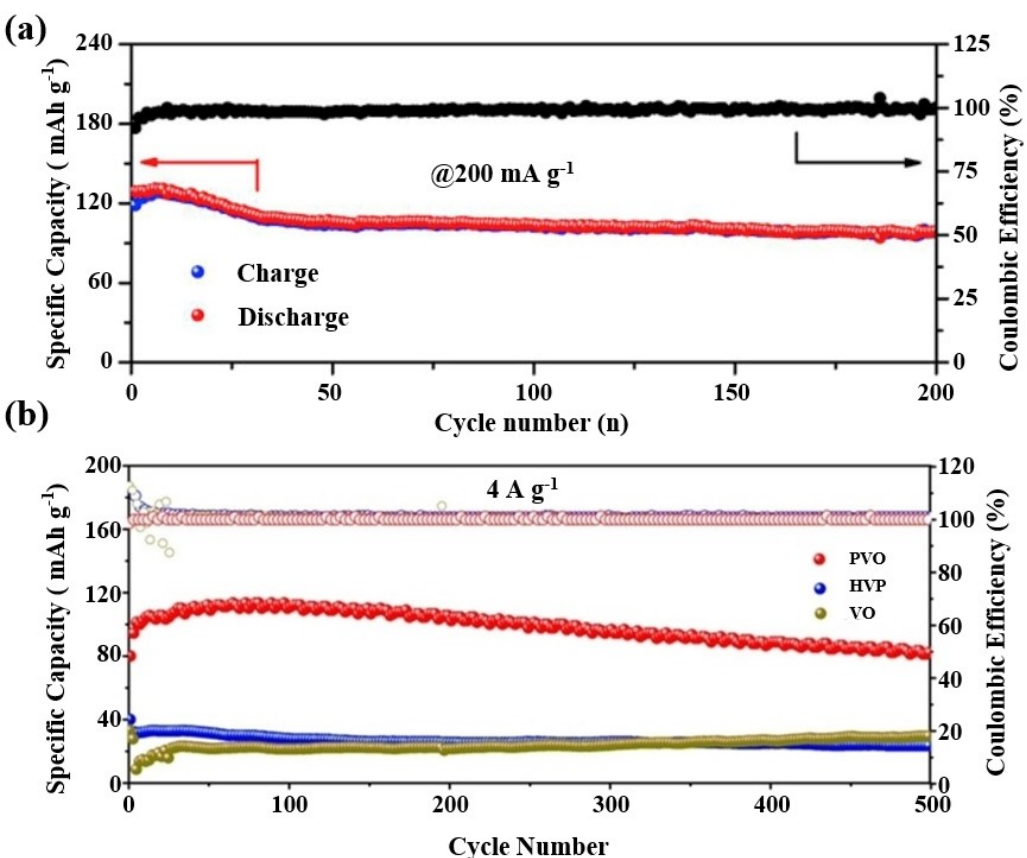


**Figure 11.** a) Cycling performance of the PTCDA. Reproduced with permission from Ref. [69]. Copyright (2019) Elsevier B.V. b) Cycling performance of PVO, HVO, and VO. Reproduced with permission from Ref. [71]. Copyright (2021) Wiley-VCH GmbH.

battery capacity, providing some guidance for the design of multivalent metal-ion batteries.

## 5. OEMs in SCBs

Calcium is widely distributed on the Earth, ranking third with the content of metal elements in the crust. As the multivalent ion, the radius of the  $\text{Ca}^{2+}$  (99 pm) cation is closer to that of  $\text{Na}^+$ , which gives it a larger radius of ion action.<sup>[75]</sup> Considering that the standard redox potential of Ca is  $-2.87 \text{ V}$  (vs. SHE), it is the lowest potential compared with that of zinc, magnesium, or aluminum, showing higher electrochemical activity. Thence, the calcium battery is extremely competitive in MSBs.<sup>[76]</sup>

As early as 1964, calcium was used as an active element in the study of primary thermal batteries.<sup>[77]</sup> However, critical issues such as high operating temperature, battery self-discharge, formation of passivation layers, and irreversibility of calcium exfoliation and electroplating in conventional electrolytes have not been effectively addressed for a long time.<sup>[78]</sup> Until recent years, with the development of new electrolytes such as  $\text{Ca}[\text{B}(\text{hfp})_4]_2$  and  $\text{Ca}[\text{B}(\text{Ohfp})_4]_2 \cdot 4\text{DME}$ , reversible Ca deposition has become a reality at room temperature.<sup>[79]</sup> Although the stability of the calcium battery needs to be improved, it opens a new avenue for developing calcium-ion batteries at room temperature. Up to date, only a few organic

materials have been reported to successfully achieve  $\text{Ca}^{2+}$  storage. Generally, organic molecules and conductive polymers containing carbonyl conjugated systems are still the dominated ones.

### 5.1. Carbonyl compounds

In 2017, a new CIB (PNDIE//CuHCF) was assembled by Ghaytani et al.<sup>[80]</sup> In the three-electrode system test, PNDIE provided an initial capacity of  $160 \text{ mAh g}^{-1}$ . Even at a current density of  $5 \text{ C}$  after 4000 cycles, PNDIE still exhibited excellent cycling stability (Coulombic efficiency close to 100) (Figure 13a). The full battery demonstrated good cycling stability as well (Figure 13b). In the same year, another example of red organic compound, 3,4,9,10-pertrasaccharide box dianhydride (PTCDA), was reported.<sup>[81]</sup> The Ca-PTCDA electrode showed a certain reversible electrochemical activity with an initial capacity of  $87 \text{ mAh g}^{-1}$ . However, the specific capacity of the battery faded rapidly. (Figure 13c).

In pursuit of high-life-time and stable SCBs, 5, 7, 12, 14-pentaenetetraone (PT) organic crystal was developed.<sup>[4c]</sup> The special channels formed within the aromatic PT crystals achieve rapid ion diffusion and effective charge transfer, so the PT electrodes show far superior doubling performance than the PTCDA, PNDIE, graphite, Sn//graphite full batteries, and Sn//AC

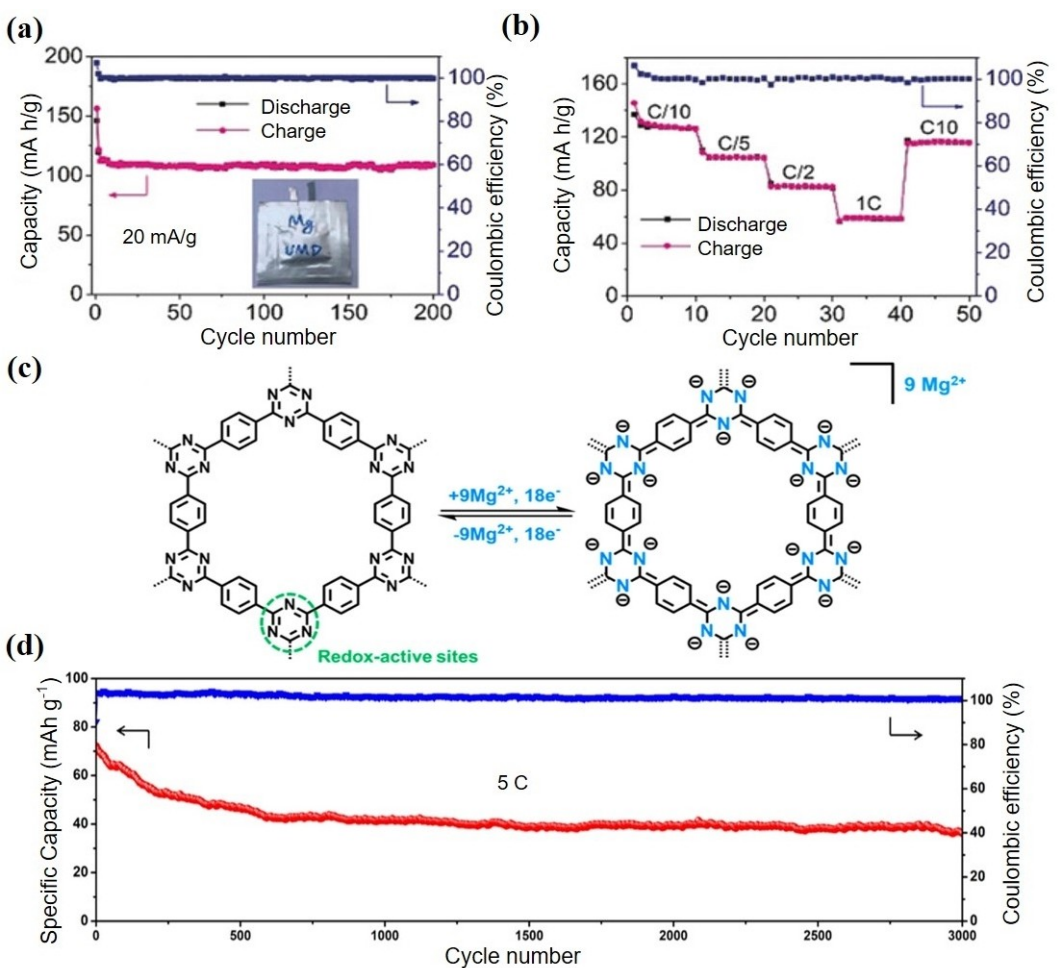


**Figure 12.** a) Cycling performance of PHATN in SMBs. b) Rate capabilities of PHATN in SMBs. Reproduced with permission from Ref. [57]. Copyright (2019) Wiley-VCH Verlag. c) Chemical structure and possible electrochemical redox mechanism of the COF. d) Cycling performance of the COF. Reproduced with permission from Ref. [72]. Copyright (2020) American Chemical Society.

full batteries. Owing to the structural characteristics of  $\pi-\pi$  coplanar stacking, the irreversible deformation of PT molecules was small with high stability during the calcium intercalation/extraction process. After 3000 cycles at  $30\text{ A g}^{-1}$ , the capacity retention rate of the PT//KCoFe(CN)<sub>6</sub> PBA full battery could still reach 81.5%.

## 5.2. Conducting polymers

The high charge density of  $\text{Ca}^{2+}$  and the strong electrostatic interaction formed between electrode materials lead to the limited capacity calcium ion storage. The ion radius of  $\text{Ca}^{2+}$  further results in slow ion diffusion, hindering the high-rate capacity of the calcium battery.<sup>[82]</sup> Therefore, it is difficult to design and synthesize organic molecules with excellent electrochemical activity and stability for SCBs. The composite modification of existing classical organic molecules is also one of the ways to improve the electrochemical activity of cathode and anode electrode materials for SCBs.

Bitenc et al. prepared nanoporous PAQS/CNTs composite cathode materials by polymerizing PAQS in the suspension of multi-walled carbon nanotubes (CNTs).<sup>[79b]</sup> This way can address the problem of low capacity of poly(anthraquinone acyl sulfide) (PAQS) in SCBs (only about 20% of the theoretical capacity of 225  $\text{mAh g}^{-1}$ ).

The first discharge capacity of PAQS/CNTs cathode reaches  $169\text{ mAh g}^{-1}$  (accounting for 75% of the theoretical capacity value). Although there was still a large capacity attenuation phenomenon in the electrode cycle process, it came up with a new concept of constructing microelectronics lines and porous structures using composite carbon nanotubes to improve the electrochemical activity of electrode materials. Similarly, the electrode material PANI/CC, which is consisted of the traditional conductive polymer polyaniline (PANI) and the coated carbon cloth, has also been disclosed for aqueous calcium ion full batteries (Figure 13d).<sup>[83]</sup> Moreover, the full battery assembled from PANI/CC also provides excellent performance (Figure 13e). Surprisingly, the SCBs could provide an energy density of  $70\text{ Wh kg}^{-1}$  at  $250\text{ W kg}^{-1}$ . Superior performance was able to

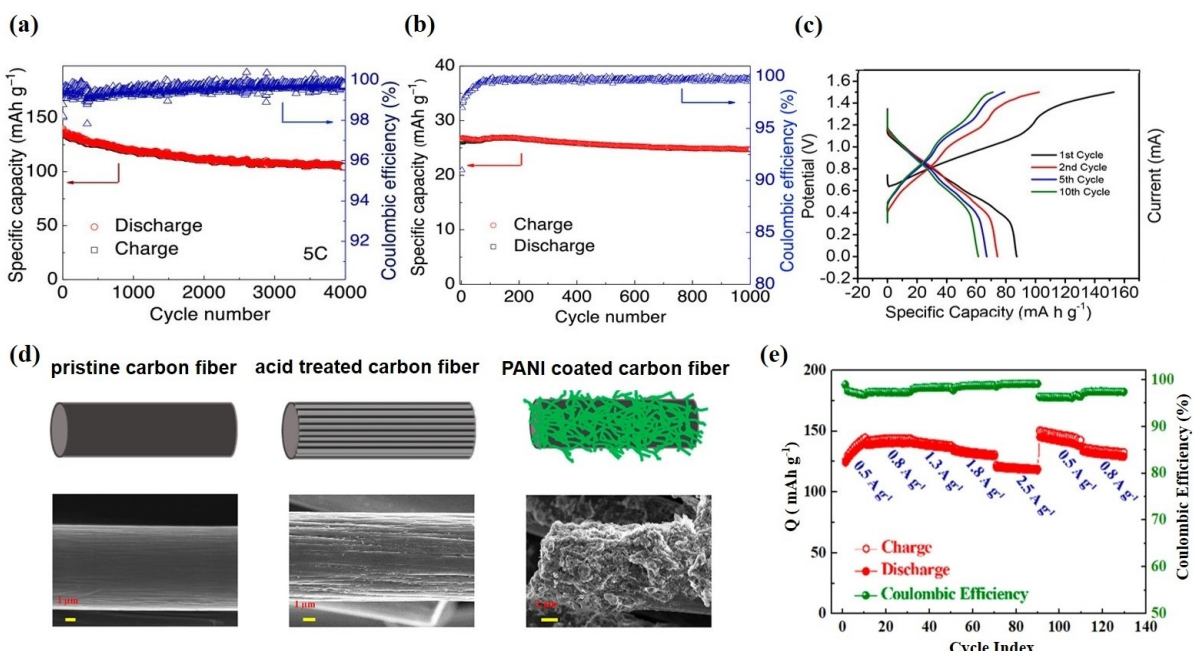


**Figure 13.** a) Cycling performance of PNDIE. b) The cycling performance of  $\text{Ca}_{0.3}\text{CuHCF}/\text{PNDIE}$  battery. Reproduced with permission from Ref. [80]. Copyright (2017) Wiley-VCH Verlag. c) Discharge-charge curves of PTCDA. Reproduced with permission from Ref. [81]. Copyright (2017) American Chemical Society. d) Schematic diagram of the preparation of polyaniline-coated carbon cloth and the corresponding SEM images. e) Rate capability of PANI/CC. Reproduced with permission from Ref. [83]. Copyright (2020) American Chemical Society.

compete with vanadium flow, lead-acid, Ni-MH, and other known full batteries.

In addition to the modification of composite carbon materials, Cang et al. prepared a novel mesoporous electrode with large specific surface area and stable structure by combining PPTCDI with molecular sieve (SBA-15).<sup>[84]</sup> The calcium ion storage capacity of the electrode is significantly affected by its mesoporous structure and enolization mechanism. The PPTCDI@SBA-15 electrode displayed a capacity of  $197 \text{ mAh g}^{-1}$ . Moreover, the SBA-15@PPTCDI ||  $\text{Ca}_2\text{MnO}_4$  full battery still exhibited a coulombic efficiency close to 100% after more than 1500 cycles.

## 6. Summary of Electrochemical Performances of OEMs in MSBs

The electrochemical properties of OEMs mentioned above are systematically summarized in Table 2. One can be easily concluded that OEMs are still dominated by organic materials containing carbonyl and imine groups. These compounds exhibit extensive adaptability in MSBs. One could also conclude that the same organic materials (such as the above-mentioned C4Q, PQ-Δ, PHATN, and so on) can be employed as electrodes in different battery systems with good compatibility activity.

In order to further improve the specific capacity and stability of organic electrodes during the cycle, the method of polymerizing small organic molecules is usually adopted, such as linear polymerization and cross-linking polymerization.

However, due to the strong interaction between highly charged ions and electrode materials, the charge transfer rate is reduced, resulting in a limited electrochemical performance of conventional stacked polymers. The examples in Table 2 provide some promising strategies: (1) Introducing rigid structures or extended conjugated structures. The introduction of the above structure can enhance the electrical conductivity of the electrode material and inhibit its dissolution, improving the battery cycle stability. (2) Constructing two-dimensional large aperture COFs. The unique large conjugated facet porous structure of COFs increases electrolyte accessibility, improves the utilization of active sites and shortens the ion diffusion path, thereby enhancing the electrochemical activity of the electrode material. (3) Composite polymers with high specific surface area or high conductivity (such as mesoporous materials, conductive carbon). The controllable microporous structure of the composite electrode materials limits the dissolution of discharge products in the electrolyte. At the same time, the enhanced electrical conductivity also endows the composite electrode material with better rate performance. (4) Introduction of heteroatoms (O, N, S). Heteroatoms have strong electronegativity, which can induce the delocalization of p electrons between benzene rings in chain or cyclic polymers, promote electron migration, and improve intrinsic conductivity. Furthermore, researches have shown the introduction of thioether bonds and ether bonds in Pillar[5]quinone (P5Q) and Calix[6]quinone (C6Q), in which O and S can be used as intercalation sites for metal ions, thereby improving the theoretical capacity of electrode materials. (5) Optimize the electrolyte system. Develop a more advantageous mixed

**Table 2.** Summary of organic compounds as effective electrodes for MSBs.

Compound <sup>[Ref.]</sup>	Structure	Counter electrode	Insertion ion	Electrolyte	Voltage Window [V]	Initial capacity [mAh g <sup>-1</sup> ]/current [mA g <sup>-1</sup> ]	Cyclability [mAh g <sup>-1</sup> ]/cycle number/current [mA g <sup>-1</sup> ]
TCBQ <sup>[26]</sup>		Zn	Zn <sup>2+</sup>	1 M Zn(CF <sub>3</sub> SO <sub>3</sub> ) <sub>2</sub>	0.5–1.5	170/43.4	83/200/217
C4Q <sup>[28,55]</sup>		Zn Al	Zn <sup>2+</sup> Al(OTf) <sup>2+</sup>	3 M Zn(CF <sub>3</sub> SO <sub>3</sub> ) <sub>2</sub> 1 M Al(OTf) <sub>3</sub>	0.2–1.8 0.4–1.4	333/50 400/40	≈115/ 1000/500 269/50/200
PTO <sup>[29a,30]</sup>		Zn	Zn <sup>2+</sup>	2 M ZnSO <sub>4</sub>	0.3–1.5	336/40	≈150/ 1000/3000
PBQS <sup>[32]</sup>		Zn	Zn <sup>2+</sup>	3 M Zn(CF <sub>3</sub> SO <sub>3</sub> ) <sub>2</sub>	0.2–1.8	203/38.8	150/50/77.6
PDBS <sup>[33a]</sup>		Zn	Zn <sup>2+</sup>	2 M ZnSO <sub>4</sub>	0.4–1.4	260/10	230/1000/ 1000
TAPQ <sup>[38]</sup>		Zn	Zn <sup>2+</sup> /H <sup>+</sup>	1 M ZnSO <sub>4</sub>	0.5–1.6	265/50	248/250/50
DTT <sup>[29b]</sup>		Zn	Zn <sup>2+</sup> /H <sup>+</sup>	2 M ZnSO <sub>4</sub>	0.3–1.4	211/50	≈78/ 23000/2000
PQ-Δ <sup>[31]</sup>		Zn Al	Zn <sup>2+</sup> / H <sub>2</sub> O Al <sup>3+</sup>	2 M Zn(CF <sub>3</sub> SO <sub>3</sub> ) <sub>2</sub> AlCl <sub>3</sub> /EMImCl = 1.3:1	0.4–1.6 0.7–1.75	225/30 110/100	≈210/500/ 150 53/5000/ 2000
HATN <sup>[35]</sup>		Zn	Zn <sup>2+</sup> /H <sup>+</sup>	2 M ZnSO <sub>4</sub>	0.3–1.1	405/100	140/5000/ 5000
HATN-3CN <sup>[36]</sup>		Zn	Zn <sup>2+</sup> /H <sup>+</sup>	2 M ZnSO <sub>4</sub>	0.1–1.6	313/50	≈280/ 5800/5000
HATNQ <sup>[37]</sup>		Zn	Zn <sup>2+</sup> /H <sup>+</sup>	3 M ZnSO <sub>4</sub>	0.1–1.6	483/200	≈195/ 11000/5000

**Table 2.** continued

Compound <sup>[Ref.]</sup>	Structure	Counter electrode	Insertion ion	Electrolyte	Voltage Window [V]	Initial capacity [mAh g <sup>-1</sup> ]/current [mA g <sup>-1</sup> ]	Cyclability [mAh g <sup>-1</sup> ]/cycle number/current [mA g <sup>-1</sup> ]
PA-COF <sup>[41]</sup>		Zn	Zn <sup>2+</sup> /H <sup>+</sup>	1 M ZnSO <sub>4</sub>	0.2–1.6	265/50	≈115/1000/1000
HqTp-COF <sup>[40]</sup>		Zn	Zn <sup>2+</sup>	3 M ZnSO <sub>4</sub>	0.2–1.8	276/125	≈81/1000/3750
HAQ-COF <sup>[42]</sup>		Zn	Zn <sup>2+</sup> /H <sup>+</sup>	2 M ZnSO <sub>4</sub>	0.2–1.6	344/100	128/10000/5000
Pth@GO <sup>[59]</sup>		Al	Al <sup>3+</sup>	AlCl <sub>3</sub> /[EMIm]Cl ionic liquid	0.1–2.4	≈130/1000	≈100/4000/1000
TCNQ <sup>[58]</sup>		Al	AlCl <sub>2</sub> <sup>+</sup> /AlCl <sub>4</sub> <sup>-</sup>	AlCl <sub>3</sub> /[EMIm]Cl ionic liquid	0–2.2	180/500	115/2000/500
G-PANI <sup>[60]</sup>		Al	Al <sup>3+</sup>	AlCl <sub>3</sub> ;1-ethyl-3-methylimidazole([EMIM]Cl)=1.3:1	0.1–2.4	160/1000	180/4000/1000
9,10-AQ <sup>[51,52,64]</sup>		Al K <sub>2</sub> CuFe(CN) <sub>6</sub>	Al <sup>3+</sup>	AlCl <sub>3</sub> ;1-ethyl-3-methylimidazoliumchloride=1.5:1	0.1–2.1	215/20	192/200/100
		Mg	Al <sup>3+</sup>	1 M Al <sub>2</sub> (SO <sub>4</sub> ) <sub>3</sub>	0.1–1.2	53/500	46/100/500
			Mg <sup>2+</sup>	0.6 M Mg(TFSI) <sub>2</sub> –2MgCl <sub>2</sub> (MTC)	0.5–2.5	152/100	12/40/100
PHATN <sup>[57]</sup>		Al Mg	Al <sup>3+</sup>	AlCl <sub>3</sub> [BMIm]Cl ionic liquid	0.2–1.2	125/50	92/200/50
			Mg <sup>2+</sup>	1 M Mg(PF <sub>6</sub> ) <sub>2</sub> /DME	0.5–2.3	146/20	110/200/20
PTCDA-SP <sup>[56]</sup>		Al	Al <sup>3+</sup>	AlCl <sub>3</sub> ;1-ethyl-3-methylimidazole([EMIM]Cl)=1.5:1	0.4–2.0	110/100	108/1200/100
TPB <sup>[54]</sup>		Al	Al <sup>3+</sup>	AlCl <sub>3</sub> /urea ionic liquid	0.2–2.5	178/100	175/250/100

**Table 2.** continued

Compound <sup>[Ref.]</sup>	Structure	Counter electrode	Insertion ion	Electrolyte	Voltage Window [V]	Initial capacity [mAh g <sup>-1</sup> ]/current [mA g <sup>-1</sup> ]	Cyclability [mAh g <sup>-1</sup> ]/cycle number/current [mA g <sup>-1</sup> ]
1,4-BQ <sup>[64]</sup>		Mg	Mg <sup>2+</sup>	0.6 M Mg(TFSI) <sub>2</sub> -2MgCl <sub>2</sub> /DME	1.0–3.0	130/100	≈38/40/100
1,4-NQ <sup>[64]</sup>		Mg	Mg <sup>2+</sup>	0.6 M Mg(TFSI) <sub>2</sub> -2MgCl <sub>2</sub> /DME	0.75–2.75	138/100	12/40/100
PAQ <sup>[68]</sup>		Mg	Mg <sup>2+</sup>	0.6 M Mg(TFSI) <sub>2</sub> -2MgCl <sub>2</sub> /DME	0.5–2.5	152/260	≈110/500/260
PMDA <sup>[65]</sup>		Mg	Mg <sup>2+</sup>	0.2 M Mg(HMDS) <sub>2</sub> -0.4 M AlCl <sub>3</sub> -0.2 M MgCl <sub>2</sub> in tetraglyme	0–2.6	110/50	45/100/50
NTCDA <sup>[65]</sup>		Mg	Mg <sup>2+</sup>	0.2 M Mg(HMDS) <sub>2</sub> -0.4 M AlCl <sub>3</sub> -0.2 M MgCl <sub>2</sub> in tetraglyme	0–2.6	130/50	90/100/50
PTCDA <sup>[69,81]</sup>		Mg Carbon	Mg <sup>2+</sup> Ca <sup>2+</sup>	1 M LiCl-APC Saturated Ca(NO <sub>3</sub> ) <sub>2</sub> aqueous solution	0.6–2.5 0–1.5	126/200 87/20	100/150/200 60/1020
PTC-S <sup>[74]</sup>		Mg	Mg <sup>2+</sup> /Li <sup>+</sup>	0.5 M MgCl <sub>2</sub> +0.5 M LiCl	−0.85–0.4	283/50	≈147/1000/1000
COF <sup>[72]</sup>		Mg	Mg <sup>2+</sup>	0.5 M Mg(TFSI) <sub>2</sub> /DME	0.8–2.5	107/22.8	≈40/3000/570
PANI/CC <sup>[83]</sup>		CuHCF	Ca <sup>2+</sup>	2.5 M Ca(NO <sub>3</sub> ) <sub>2</sub>	0.2–1.0	130/800	≈124/200/800
PAQS/CNTs <sup>[79b]</sup>		Ca	Ca <sup>2+</sup>	0.3 M Ca[B(hfip) <sub>4</sub> ] <sub>2</sub>	1.3–3.3	169/112.5	114/10/112.5
PT <sup>[4c]</sup>		KCoFe(CN) <sub>6</sub> -PBA	Ca <sup>2+</sup> /H <sup>+</sup>	1 M CaCl <sub>2</sub>	0–2.1	151/5000	≈56/3000/30000
PNDIE <sup>[80]</sup>		CuHCF	Ca <sup>2+</sup>	2.5 M Ca(NO <sub>3</sub> ) <sub>2</sub>	0.5–1.9	27/400	≈24/1000/400
PPTCDI@SBA-15 <sup>[84]</sup>		Ca <sub>2</sub> MnO <sub>4</sub>	Ca <sup>2+</sup>	1 M Ca(NO <sub>3</sub> ) <sub>2</sub>	0–1.8	122/100	≈110/800/100

electrolyte system to achieve fast reaction kinetics, stable charge-discharge platform, or give batteries better temperature adaptability.

## 7. Conclusion and Prospects

We have reviewed the recent progress of various OEMs in multivalent (Zn, Al, Mg, Ca) secondary batteries. OEMs have many advantages over traditional IEMs including their renewability, diversified structures, and abound resources, which have been widely used in MSBs. The current research on OEMs in MSBs mainly focuses on electrochemical performance improvement, energy storage mechanism exploration, and system compatibility matching. For instance, the few active sites and poor reversibility of some small molecular organic materials become the hindering factors. How to improve the electrochemical properties through modification, polymerization or composites is an important topic. Besides, with the continuous advances in analytical techniques and theoretical computational methods, the mechanism of H<sup>+</sup>-assisted energy storage has gradually been recognized. Subsequently, the mechanism of the participation of AlCl<sub>2</sub><sup>+</sup>, AlCl<sub>4</sub><sup>-</sup>, Al(OTf)<sub>2</sub><sup>+</sup> plasma in the energy storage of SABs has also been successively revealed. The proposal of an energy storage mechanism provides great guidance for OEMs to be adapted to appropriate electrolyte systems.

Although the application of OEMs in MSBs shows great development prospects, it also faces many challenges: (1) The actual specific capacity of OEMs in MSBs is low, resulting in the limited energy density of organic MSBs. Even though the specific capacity of OEMs in MSBs has been significantly improved in recent years, the energy density is still lower than the dominant inorganic counterpart. The influence comes from many aspects: i) Most OEMs have low intrinsic conductivity. To improve their conductivity, a larger proportion of conductive carbon and binder is usually mixed, but this reduces the energy density of the OEMs. ii) In pursuit of high-capacity OEMs, organic molecular polymerization is an efficient method. However, due to the low conductivity and slow reaction kinetics of the polymer, its actual capacity is lower than the theoretical capacity. iii) By compositing inorganic materials (such as coating and other methods), the dissolution of OEMs can be limited and the stability of MSBs can be improved during charge and discharge. However, the energy density of OEMs is also reduced. iv) Different from singly charged ions (Li<sup>+</sup>, Na<sup>+</sup>, K<sup>+</sup>), multivalent ions (Zn<sup>2+</sup>, Al<sup>3+</sup>, Mg<sup>2+</sup>, Ca<sup>2+</sup>) need to combine with two or three adjacent active sites on the OEMs to achieve intercalation during discharge. This often results in a large number of active sites not being utilized, making the actual capacity of the MSBs much lower than the theoretical capacity. (2) Compared with commercial LIBs, the voltage range of OEMs at MSBs is narrow and the reaction potential is low, which greatly limits their practical application. Therefore, rational design of OEMs with more reactive groups and electron-withdrawing groups should be considered to improve the output voltage of MSBs. (3) Notably, only SZBs can work

with the water-electrolyte system between MSBs. Other MSBs (Al, Mg, Ca) have a great dependence on some special non-aqueous electrolytes, such as ionic liquids, and mixed organic electrolytes. It is urgent to develop electrolytes with strong adaptability, cheapness, and excellent performance as well. (4) The occurrence of side effects and the growth of dendrites remain serious problems plaguing MSBs. Especially for ASZBs, although high ion transport rates are obtained in aqueous electrolytes, they are also accompanied by more serious side reactions and zinc dendrite growth. How to solve such problems has become a hot field of current zinc battery research.

In conclusion, the research of OEMs in MSBs is accompanied by opportunities and challenges. In the future, while focusing on improving and optimizing the performance of electrode materials, MSBs can be used as an energy storage device for solar energy, wind energy, tidal energy, and other intermittent energy sources by virtue of the advantages of a wide range of raw materials, safety, and environmental protection. In addition, the successful development of many flexible MSBs has laid a solid foundation for the application of MSBs in foldable and wearable devices as well. It is believed that MSBs will also inject new power into the new energy market with the rapid development of emerging technologies in various fields.

## Acknowledgements

This work was financially supported by the financial support of the National Natural Science Foundation of China (No. 21875206, 21403187). Q. Z. thanks the funding support from City University of Hong Kong and Hong Kong Institute for Advanced Study, City University of Hong Kong.

## Conflict of Interest

The authors declare no conflict of interest.

**Keywords:** molecular engineering · multivalent metal ions · multivalent metal · organic electrodes · secondary batteries

- [1] a) H. Guo, H. Yu, P. Liu, Y. Ren, T. Zhang, M. Chen, M. Ishida, H. Zhou, *Energy Environ. Sci.* **2015**, *8*, 1237–1244; b) Y. Tong, Z. Sun, J. Wang, W. Huang, Q. Zhang, *SmartMat.* **2022**, DOI: 10.1002/smm.2.1115; c) W. Huang, S. Liu, C. Li, Y. Lin, P. Hu, Z. Sun, Q. Zhang, *EcoMat.* **2022**, DOI: 10.1002/eom2.12214.
- [2] a) Y. Liang, Y. Jing, S. Gheytani, K. Lee, P. Liu, A. Facchetti, Y. Yao, *Nat. Mater.* **2017**, *16*, 841; b) J. B. Goodenough, A. Manthiram, *MRS Commun.* **2014**, *4*, 135–142.
- [3] a) J. Wu, X. Rui, G. Long, W. Chen, Q. Yan, Q. Zhang, *Angew. Chem. Int. Ed.* **2015**, *54*, 7354–7358; *Angew. Chem.* **2015**, *127*, 7462–7466; b) Q. Zhang, J. Niu, Z. Zhao, Q. Wang, *J. Energy Storage Mater.* **2022**, *45*, 103759; c) X. Li, R. Zhao, Y. Fu, A. Manthiram, *eScience* **2021**, *1*, 108–123; d) Y. Zhang, Z. Sun, X. Kong, Y. Lin, W. Huang, *J. Mater. Chem. A* **2021**, *9*, 26208–26215; e) C.-J. Yao, Z. Wu, J. Xie, F. Yu, W. Guo, Z. Xu, D.-S. Li, S. Zhang, Q. Zhang, *ChemSusChem* **2020**, *13*, 2457; f) Z. Wu, D. Adekoya, X. Huang, M. J. Kiefel, J. Xie, W. Xu, Q. Zhang, D. Zhu, S. Zhang, *ACS Nano* **2020**, *14*, 12016–12026.

- [4] a) Y. Huang, Z. Chang, W. Liu, W. Huang, L. Dong, F. Kang, C. Xu, *Chem. Eng. J.* **2022**, *431*, 133902; b) J. Han, Z. Chen, J. Xu, J. Han, *Mater. Lett.* **2021**, *304*, 130629; c) C. Han, H. Li, Y. Li, J. Zhu, C. Zhi, *Nat. Commun.* **2021**, *12*, 1–12.
- [5] a) N. Li, Y. Yao, T. Lv, Z. Chen, Y. Yang, S. Cao, T. Chen, *J. Power Sources* **2021**, *488*, 229460; b) Z. Tong, R. Lian, R. Yang, T. Kang, J. Feng, D. Shen, Y. Wu, X. Cui, H. Wang, Y. Tang, C. Lee, *Energy Storage Mater.* **2022**, *44*, 497–507; c) L. Dong, R. Xu, P. Wang, S. Sun, Y. Li, L. Zhen, C. Xu, *J. Power Sources* **2020**, *479*, 228793; d) M. Asif, S. Kilian, M. Rashad, *Energy Storage Mater.* **2021**, *42*, 129–144; e) J. Xie, Q. Zhang, *Small* **2019**, *15*, 1805061.
- [6] a) Y. Yang, H. Yang, X. Wang, Y. Bai, C. Wu, *J. Energy Chem.* **2022**, *64*, 144–165; b) N. Fu, Y. Xu, S. Zhang, Q. Deng, J. Liu, C. Zhou, X. Wu, Y. Guo, X. Zeng, *J. Energy Chem.* **2022**, *67*, 563–584.
- [7] a) A. I. Volkov, A. S. Sharlaev, O. Ya Berezina, E. G. Tolstopiatova, L. Fu, V. V. Kondratiev, *Mater. Lett.* **2022**, *308*, 131212; b) Z. Wang, P. Liang, R. Zhang, Z. Liu, W. Li, Z. Pan, H. Yang, X. Shen, J. Wang, *Appl. Surf. Sci.* **2021**, *562*, 150196.
- [8] a) P. Almodóvar, D. Giraldo, C. Díaz-Guerra, J. Ramírez-Castellanos, J. M. González Calbet, J. Chacón, M. L. López, *J. Power Sources* **2021**, *516*, 230656; b) T. Tojo, H. Tawa, N. Oshida, R. Inada, Y. Sakurai, *J. Electroanal. Chem.* **2018**, *825*, 51–56; c) Y. Deng, X. Tong, N. Pang, Y. Zhou, D. Wu, S. Xu, D. Xiong, L. Wang, P. Chu, *Appl. Surf. Sci.* **2022**, *572*, 151442; d) F. Zhu, H. Zhang, Z. Lu, D. Kang, L. Han, *J. Energy Storage* **2021**, *42*, 103046.
- [9] a) R. Sun, L. Zhang, J. Feng, K. Fang, A. Wang, *J. Colloid Interface Sci.* **2022**, *608*, 2100–2110; b) J. Y. Lee, G. D. Park, J. H. Kim, J. H. Hong, Y. C. Kang, *Int. J. Energy Res.* **2021**, *45*, 16091–16101.
- [10] a) H. Shang, Z. Zhang, C. Liu, X. Zhang, S. Li, Z. Wen, S. Ji, J. Sun, *J. Electroanal. Chem.* **2021**, *890*, 115253; b) X. Cao, L. Wang, J. Chen, J. Zheng, *ChemElectroChem* **2018**, *5*, 2789–2794; c) S. Islam, M. H. Alfaruqi, D. Y. Putro, S. Park, S. Kim, S. Lee, M. S. Ahmed, V. Mathew, Y. K. Sun, J. Y. Hwang, J. Kim, *Adv. Sci.* **2021**, *8*, 2002636.
- [11] a) H. Yi, R. Qin, S. Ding, Y. Wang, S. Li, Q. Zhao, F. Pan, *Adv. Funct. Mater.* **2021**, *31*, 2006970; b) G. Zampardi, F. L. Mantia, *Curr. Opin. Electrochem.* **2020**, *21*, 84–92; c) L. Cui, M. Chen, G. Huo, X. Fu, J. Luo, *Chem. Eng. J.* **2020**, *395*, 125158.
- [12] a) M. Tang, Q. Zhu, P. Hu, L. Jiang, R. Liu, J. Wang, L. Cheng, X. Zhang, W. Chen, H. Wang, *Adv. Funct. Mater.* **2021**, *31*, 2102011; b) Y. Bai, C. Liu, T. Chen, W. Li, S. Zheng, Y. Pi, Y. Luo, H. Pang, *Angew. Chem. Int. Ed.* **2021**, *60*, 25318–25322.
- [13] a) D. Xu, H. Zhang, L. Zhou, X. Gao, X. Lu, *ChemPhysMater* **2021**, *1*, 86–101; b) M. Zhang, W. Zhou, W. Huang, *J. Energy Chem.* **2021**, *57*, 291–303.
- [14] a) K. Qin, J. Huang, K. Holguin, C. Luo, *Energy Environ. Sci.* **2020**, *13*, 3950–3992; b) J. Ming, J. Guo, C. Xia, W. Wang, H. N. Alshareef, *Mat. Sci. Eng. R. Rep.* **2019**, *135*, 58–84.
- [15] a) J. J. Shea, C. Luo, *ACS Appl. Mater. Interfaces* **2020**, *12*, 5361–5380; b) Q. Cheng, X. Zhao, G. Yang, L. Mao, F. Liao, L. Chen, P. He, D. Pan, S. Chen, *Energy Storage Mater.* **2021**, *41*, 842–882.
- [16] P. Canepa, G. Sai Gautam, D. C. Hannah, R. Malik, M. Liu, K. G. Gallagher, K. A. Persson, G. Ceder, *Chem. Rev.* **2017**, *117*, 4287–4341.
- [17] D. Chao, W. Zhou, F. Xie, C. Ye, H. Li, M. Jaroniec, S. Qiao, *Sci. Adv.* **2020**, *6*, eaaba4098.
- [18] M. Winter, R. J. Brodd, *Chem. Rev.* **2004**, *104*, 4245–4270.
- [19] a) T. Sun, H. J. Fan, *Curr. Opin. Electrochem.* **2021**, *30*, 100799; b) A. Konarov, N. Voronina, J. H. Jo, Z. Bakenov, Y.-K. Sun, S.-T. Myung, *ACS Energy Lett.* **2018**, *3*, 2620–2640.
- [20] S. Zheng, Q. Wang, Y. Hou, L. Li, Z. Tao, *J. Energy Chem.* **2021**, *63*, 87–112.
- [21] N. Wang, R. Zhou, H. Li, Z. Zheng, W. Song, T. Xin, M. Hu, J. Liu, *ACS Energy Lett.* **2021**, *6*, 1141–1147.
- [22] H. Shi, Y. Ye, K. Liu, Y. Song, X. Sun, *Angew. Chem. Int. Ed.* **2018**, *57*, 16359–16363; *Angew. Chem.* **2018**, *130*, 16597–16601.
- [23] a) S. Liu, H. Zhu, B. Zhang, G. Li, H. Zhu, Y. Ren, H. Geng, Y. Yang, Q. Liu, C. Li, *Adv. Mater.* **2020**, *32*, e2001113; b) M. Wang, J. Zhang, L. Zhang, J. Li, W. Wang, Z. Yang, L. Zhang, Y. Wang, J. Chen, Y. Huang, D. Mitlin, X. Li, *ACS Appl. Mater. Interfaces* **2020**, *12*, 31564–31574.
- [24] S. Zhang, S. Long, H. Li, Q. Xu, *Chem. Eng. J.* **2020**, *400*, 125898.
- [25] P. Poizot, J. Gaubicher, S. Renault, L. Dubois, Y. Liang, Y. Yao, *Chem. Rev.* **2020**, *120*, 6490–6557.
- [26] D. Kundu, P. Oberholzer, C. Glaros, A. Bouzid, E. Tervoort, A. Pasquarello, M. Niederberger, *Chem. Mater.* **2018**, *30*, 3874–3881.
- [27] a) H. Sun, X. Zhang, M. Zhang, J. Lv, L. Wang, W. Huang, *Org. Electron.* **2020**, *87*, 105966; b) W. Zhou, X. Zhang, W. Zhang, W. Huang, B. Yan, H. Li, S. Yu, *Org. Electron.* **2020**, *82*, 105702.
- [28] Q. Zhao, W. Huang, Z. Luo, L. Liu, Y. Lu, Y. Li, L. Li, J. Hu, H. Ma, J. Chen, *Sci. Adv.* **2018**, *4*, eaao1760.
- [29] a) Z. Guo, Y. Ma, X. Dong, J. Huang, Y. Wang, Y. Xia, *Angew. Chem. Int. Ed.* **2018**, *57*, 11737–11741; *Angew. Chem.* **2018**, *130*, 11911–11915; b) Y. Wang, C. Wang, Z. Ni, Y. Gu, B. Wang, Z. Guo, Z. Wang, D. Bin, J. Ma, Y. Wang, *Adv. Mater.* **2020**, *32*, e2000338.
- [30] T. Sun, S. Zheng, H. Du, Z. Tao, *Nano-Micro Lett.* **2021**, *13*, 204.
- [31] K. W. Nam, H. Kim, Y. Beldjoudi, T. W. Kwon, D. J. Kim, J. F. Stoddart, *J. Am. Chem. Soc.* **2020**, *142*, 2541–2548.
- [32] G. Dawut, Y. Lu, L. Miao, J. Chen, *Inorg. Chem. Front.* **2018**, *5*, 1391–1396.
- [33] a) T. Sun, Z. Li, Y. Zhi, Y. Huang, H. Fan, Q. Zhang, *Adv. Funct. Mater.* **2021**, *31*, 2010049; b) J. Xie, F. Yu, J. Zhao, W. Guo, H.-L. Zhang, G. Cui, Q. Zhang, *Energy Storage Mater.* **2020**, *33*, 283; c) W. Yang, X. Du, J. Zhao, Z. Chen, J. Li, J. Xie, Y. Zhang, Z. Cui, Q. Kong, Z. Zhao, C. Wang, Q. Zhang, G. Cui, *Joule* **2020**, *4*, 1557.
- [34] K. Liu, J. Zheng, G. Zhong, Y. Yang, *J. Mater. Chem.* **2011**, *21*, 4125–4131.
- [35] Z. Tie, L. Liu, S. Deng, D. Zhao, Z. Niu, *Angew. Chem. Int. Ed.* **2020**, *59*, 4920–4924; *Angew. Chem.* **2020**, *132*, 4950–4954.
- [36] Z. Ye, S. Xie, Z. Cao, L. Wang, D. Xu, H. Zhang, J. Matz, P. Dong, H. Fang, J. Shen, M. Ye, *Energy Storage Mater.* **2021**, *37*, 378–386.
- [37] S. Zheng, D. Shi, D. Yan, Q. Wang, T. Sun, T. Ma, L. Lin, D. He, Z. Tao, J. Chen, *Angew. Chem. Int. Ed.* **2022**, *134*, e202117511.
- [38] Y. Gao, G. Li, F. Wang, J. Chu, P. Yu, B. Wang, H. Zhan, Z. Song, *Energy Storage Mater.* **2021**, *40*, 31–40.
- [39] a) W. Zhang, W. Huang, Q. Zhang, *Chem. Eur. J.* **2021**, *27*, 6131–6144; b) S. Li, Y. Liu, L. Dai, S. Li, B. Wang, J. Xie, P. Li, *Energy Storage Mater.* **2022**, *48*, 439–446; c) M. Li, Y. Wang, S. Sun, Y. Yang, G. Gu, Z. Zhang, *Chem. Eng. J.* **2022**, *429*, 132254; d) T. Sun, J. Xie, W. Guo, D.-S. Li, Q. Zhang, *Adv. Energy Mater.* **2020**, *10*, 1904199; e) X. Zhan, Z. Chen, Q. Zhang, *J. Mater. Chem. A* **2017**, *5*, 14463–14479.
- [40] A. Khayum, M. M. Ghosh, V. Vijayakumar, A. Halder, M. Nurhuda, S. Kumar, M. Addicoat, S. Kurungot, R. Banerjee, *Chem. Sci.* **2019**, *10*, 8889–8894.
- [41] W. Wang, V. S. Kale, Z. Cao, S. Kandambeth, W. Zhang, J. Ming, P. T. Parvatkar, E. Abou-Hamad, O. Shekhah, L. Cavallo, M. Eddaoudi, H. N. Alshareef, *ACS Energy Lett.* **2020**, *5*, 2256–2264.
- [42] W. Wang, V. S. Kale, Z. Cao, Y. Lei, S. Kandambeth, G. Zou, Y. Zhu, E. Abouhamad, O. Shekhah, L. Cavallo, M. Eddaoudi, H. N. Alshareef, *Adv. Mater.* **2021**, *33*, e2103617.
- [43] a) Z. Liu, X. Wang, Z. Liu, S. Zhang, Z. Lv, Y. Cui, L. Du, K. Li, G. Zhang, M. Lin, H. Du, *ACS Appl. Mater. Interfaces* **2021**, *13*, 28164–28170; b) M. Chiku, H. Takeda, S. Matsumura, E. Higuchi, H. Inoue, *ACS Appl. Mater. Interfaces* **2015**, *7*, 24385–24389; c) M. Chiku, H. Takeda, Y. Yamaguchi, E. Higuchi, H. Inoue, *Int. J. Chem.* **2013**, *5*, 1–8.
- [44] S. Das, S. Manna, B. Pathak, *ACS Omega* **2021**, *6*, 1043–1053.
- [45] a) F. Ambroz, T. J. Macdonald, T. Nann, *Adv. Energy Mater.* **2017**, *7*, 1602093; b) Y. Zhang, S. Liu, Y. Ji, J. Ma, H. Yu, *Adv. Mater.* **2018**, *30*, 1706310.
- [46] a) S. S. Manna, P. Bhauriyal, B. Pathak, *Mater. Adv.* **2020**, *1*, 1354–1363; b) N. Canever, N. Bertrand, T. Nann, *Chem. Commun.* **2018**, *54*, 11725–11728; c) W. Zhou, M. Zhang, X. Kong, W. Huang, Q. Zhang, *Adv. Sci.* **2021**, *8*, 2004490.
- [47] a) Y. Hu, B. Luo, D. Ye, X. Zhu, M. Lyu, L. Wang, *Adv. Mater.* **2017**, *29*, 1606132; b) S. Wang, Z. Yu, J. Tu, J. Wang, D. Tian, Y. Liu, S. Jiao, *Adv. Energy Mater.* **2016**, *6*, 1600137; c) S. Wang, S. Jiao, J. Wang, H. Chen, D. Tian, H. Lei, D. Fang, *ACS Nano* **2017**, *11*, 469–477; d) J. Liu, Z. Li, X. Huo, J. Li, *J. Power Sources* **2019**, *422*, 49–56; e) H. Li, H. Yang, Z. Sun, Y. Shi, H. Cheng, F. Li, *Nano Energy* **2019**, *56*, 100–108; f) S. Zheng, Y. Sun, H. Xue, P. Braunstein, W. Huang, H. Pang, *Natl. Sci. Rev.* **2021**, DOI:10.1093/nsr/nwab197.
- [48] a) C. Liu, Y. Bai, W. Li, F. Yang, G. Zhang, H. Pang, *Angew. Chem. Int. Ed.* **2022**, *61*, e202116282; b) S. Zheng, Q. Li, H. Xue, H. Pang, Q. Xu, *Natl. Sci. Rev.* **2020**, *7*, 305–314.
- [49] a) V. Raju, V. N. K. Y. V. R. Jetti, P. Basak, *ACS Appl. Energ. Mater.* **2021**, *4*, 9227–9239.
- [50] X. Xiao, M. Wang, J. Tu, Y. Luo, S. Jiao, *ACS Sustain. Chem. Eng.* **2019**, *7*, 16200–16208.
- [51] L. Zhou, Z. Zhang, F. Xiong, Q. An, Z. Zhou, X. Yu, P. K. Chu, K. Zhang, *Cell Rep. Phys. Sci.* **2021**, *2*, 100354.

- [52] L. Yan, X. Zeng, S. Zhao, W. Jiang, Z. Li, X. Gao, T. Liu, Z. Ji, T. Ma, M. Ling, C. Liang, *ACS Appl. Mater. Interfaces* **2021**, *13*, 8353–8360.
- [53] D. J. Kim, D. J. Yoo, M. T. Otley, A. Prokofjevs, C. Pezzato, M. Owczarek, S. J. Lee, J. W. Choi, J. F. Stoddart, *Nat. Energy* **2019**, *4*, 51.
- [54] Y. Kao, S. Patil, C. An, S. Huang, J. Lin, T. Lee, Y. Lee, H. Chou, C. Chen, Y. Chang, Y. Lai, D. Wang, *ACS Appl. Mater. Interfaces* **2020**, *12*, 25853–25860.
- [55] Y. Li, L. Liu, Y. Lu, R. Shi, Y. Ma, Z. Yan, K. Zhang, J. Chen, *Adv. Funct. Mater.* **2021**, *31*, 2102063.
- [56] L. Fang, L. Zhou, L. Cui, P. Jiao, Q. An, K. Zhang, *J. Energy Chem.* **2021**, *63*, 320–327.
- [57] M. Mao, C. Luo, T. P. Pollard, S. Hou, T. Gao, X. Fan, C. Cui, J. Yue, Y. Tong, G. Yang, T. Deng, M. Zhang, J. Ma, L. Suo, O. Borodin, C. Wang, *Angew. Chem. Int. Ed.* **2019**, *58*, 17820–17826; *Angew. Chem.* **2019**, *131*, 17984–17990.
- [58] F. Guo, Z. Huang, M. Wang, W. Song, A. Lv, X. Han, J. Tu, S. Jiao, *Energy Storage Mater.* **2020**, *33*, 250–257.
- [59] D. Kong, H. Fan, X. Ding, D. Wang, S. Tian, H. Hu, D. Du, Y. Li, X. Gao, H. Hu, Q. Xue, Z. Yan, H. Ren, W. Xing, *ACS Appl. Mater. Interfaces* **2020**, *12*, 46065–46072.
- [60] D. Wang, H. Hu, Y. Liao, D. Kong, T. Cai, X. Gao, H. Hu, M. Wu, Q. Xue, Z. Yan, H. Ren, W. Xing, *Sci. China Mater.* **2021**, *64*, 318–328.
- [61] a) Y. Wang, Z. Liu, C. Wang, Y. Hu, H. Lin, W. Kong, J. Ma, Z. Jin, *Energy Storage Mater.* **2020**, *26*, 494–502; b) M. Mao, X. Ji, S. Hou, T. Gao, F. Wang, L. Chen, X. Fan, J. Chen, J. Ma, C. Wang, *Chem. Mater.* **2019**, *31*, 3183–3191.
- [62] a) J. Yin, A. B. Brady, E. S. Takeuchi, A. C. Marschilok, K. J. Takeuchi, *Chem. Commun.* **2017**, *53*, 3665–3668; b) H. Sano, H. Senoh, M. Yao, H. Sakaebe, T. Kiyobayashi, *Chem. Lett.* **2012**, *41*, 1594–1596.
- [63] B. Pan, D. Zhou, J. Huang, L. Zhang, A. K. Burrell, J. T. Vaughey, Z. Zhang, C. Liao, *J. Electrochem. Soc.* **2016**, *163*, A580–A583.
- [64] J. Bitenc, T. Pavcnik, U. Kosir, K. Pirnat, *Materials* **2020**, *13*, 506.
- [65] H. Yang, F. Xu, *ChemPhysChem* **2021**, *22*, 1455–1460.
- [66] Y. Xiu, Z. Li, V. Bhaghavathi Parambath, Z. Ding, L. Wang, A. Reupert, M. Fichtner, Z. Zhao-Karger, *Batteries & Supercaps* **2021**, *4*, 1850–1857.
- [67] B. Pan, J. Huang, Z. Feng, L. Zeng, M. He, L. Zhang, J. T. Vaughey, M. J. Bedzyk, P. Fenter, Z. Zhang, A. K. Burrell, C. Liao, *Adv. Energy Mater.* **2016**, *6*, 1600140.
- [68] J. Bitenc, K. Pirnat, E. Žagar, A. Randon-Vitanova, R. Dominko, *J. Power Sources* **2019**, *430*, 90–94.
- [69] L. Cui, L. Zhou, K. Zhang, F. Xiong, S. Tan, M. Li, Q. An, Y. Kang, L. Mai, *Nano Energy* **2019**, *65*, 103902.
- [70] K. Wang, H. Wu, Y. Meng, Z. Wei, *Small* **2014**, *10*, 14–31.
- [71] C. Zuo, Y. Xiao, X. Pan, F. Xiong, W. Zhang, J. Long, S. Dong, Q. An, P. Luo, *ChemSusChem* **2021**, *14*, 2093–2099.
- [72] R. Sun, S. Hou, C. Luo, X. Ji, L. Wang, L. Mai, C. Wang, *Nano Lett.* **2020**, *20*, 3880–3888.
- [73] J. Zhang, L. Kong, L. Zhan, J. Tang, H. Zhan, Y. Zhou, C. Zhan, *J. Power Sources* **2007**, *168*, 278–281.
- [74] R. Cang, K. Ye, S. Shao, K. Zhu, J. Yan, G. Wang, D. Cao, *Chem. Eng. J.* **2021**, *405*, 126783.
- [75] M. Elena Arroyo-de Dompablo, A. Ponrouch, P. Johansson, M. Rosa Palacin, *Chem. Rev.* **2020**, *120*, 6331–6357.
- [76] L. Stievano, I. de Meatza, J. Bitenc, C. Cavallo, S. Brutt, M. A. Navarra, *J. Power Sources* **2021**, *482*, 228875.
- [77] S. M. Selis, J. P. Wondowski, R. F. Justus, *J. Electrochem. Soc.* **1964**, *111*, 6–13.
- [78] a) R. J. Staniewicz, *J. Electrochem. Soc.* **1980**, *127*, 782–789; b) E. Peled, A. Meitav, M. Brand, *J. Electrochem. Soc.* **1981**, *128*, 1936–1938; c) D. Aurbach, R. Skaletsky, Y. Gofer, *J. Electrochem. Soc.* **1991**, *138*, 3536.
- [79] a) A. Ponrouch, D. Tchitchevko, C. Frontera, F. Bardé, M. E. Arroyo-de Dompablo, M. R. Palacín, *Electrochem. Commun.* **2016**, *66*, 75–78; b) J. Bitenc, A. Scafuri, K. Pirnat, M. Lozinšek, I. Jerman, J. Grdadolnik, B. Fraisse, R. Berthelot, L. Stievano, R. Dominko, *Batteries & Supercaps* **2021**, *4*, 214–220.
- [80] S. Gheytani, Y. Liang, F. Wu, Y. Jing, H. Dong, K. K. Rao, X. Chi, F. Fang, Y. Yao, *Adv. Sci.* **2017**, *4*, 1700465.
- [81] I. A. Rodríguez-Pérez, Y. Yuan, C. Bommier, X. Wang, L. Ma, D. P. Leonard, M. M. Lerner, R. G. Carter, T. Wu, P. A. Greaney, J. Lu, X. Ji, *J. Am. Chem. Soc.* **2017**, *139*, 13031–13037.
- [82] a) Y. Cao, K. Sharma, A. A. Rajhi, S. Alamri, A. E. Anqi, A. S. El-Shafay, A. A. Aly, B. F. Felemban, S. Rashidi, M. Derakhshan, *J. Electroanal. Chem.* **2022**, *910*, 115929; b) A. P. Black, C. Frontera, A. Torres, M. Recio-Poo, P. Rozier, J. D. Forero-Saboya, F. Fauth, E. Urones-Garrote, M. E. Arroyo-de Dompablo, M. R. Palacín, *Energy Storage Mater.* **2022**, *47*, 354–364.
- [83] M. Adil, A. Sarkar, A. Roy, M. R. Panda, A. Nagendra, S. Mitra, *ACS Appl. Mater. Interfaces* **2020**, *12*, 11489–11503.
- [84] R. Cang, C. Zhao, K. Ye, J. Yin, K. Zhu, J. Yan, G. Wang, D. Cao, *ChemSusChem* **2020**, *13*, 3911–3918.

Manuscript received: April 3, 2022

Revised manuscript received: May 1, 2022

Accepted manuscript online: May 9, 2022

Version of record online: May 24, 2022